Udine University, February 23rd 2007

PhD Thesis Defense

INDIRECT SEARCH OF DARK MATTER IN THE HALOS OF GALAXIES

Role of substructures on the signals from dark matter annihilation and prospects for detection of a single dark matter clump with the MAGIC Telescope

ERICA BISESI

Index:

- deep investigation into DM distribution:
  - dynamical evolution of DM substructures
  - subhalo spatial mass function
- enhancement from subhalos in γ and cosmic-ray signals
- Is there a chance to identify a single DM clump?
  - the case of the unidentified EGRET source 3EG_J1835+5918
- MAGIC data analysis:
  - data analysis of 3EG_J1835+5918
    - ($\rightarrow$ after calibration analysis of the Crab Nebula)
- TeV emission from galaxies:
  - the Draco dwarf spheroidal
  - the baryonic versus DM luminosity of star-forming galaxies
  - M31: the Andromeda galaxy

Substructures in galaxies and clusters of galaxies

Standard cosmological picture:

- Formation and evolution of structures occur in a hierarchical framework;
- DM halos arise from the gravitational amplification of primeval fluctuations, generated at the epoch of inflation with a primordial power spectrum;
- halos are not smooth structureless objects, but clumpy systems characterized by the presence of a wide population of subhalos.

- WIMPs scenario:
  - Fluctuations are imposed for a SUSY model with a particle mass $m_\chi = 100$ GeV;
- the first objects to form have mass of $10^{-6}\,M_\odot$ and half mass radii of 10^{-2} pc;
- they are stable against gravitational disruption;
- we expect $\geq 10^{15}$ subhalos to survive within the Galactic halo.

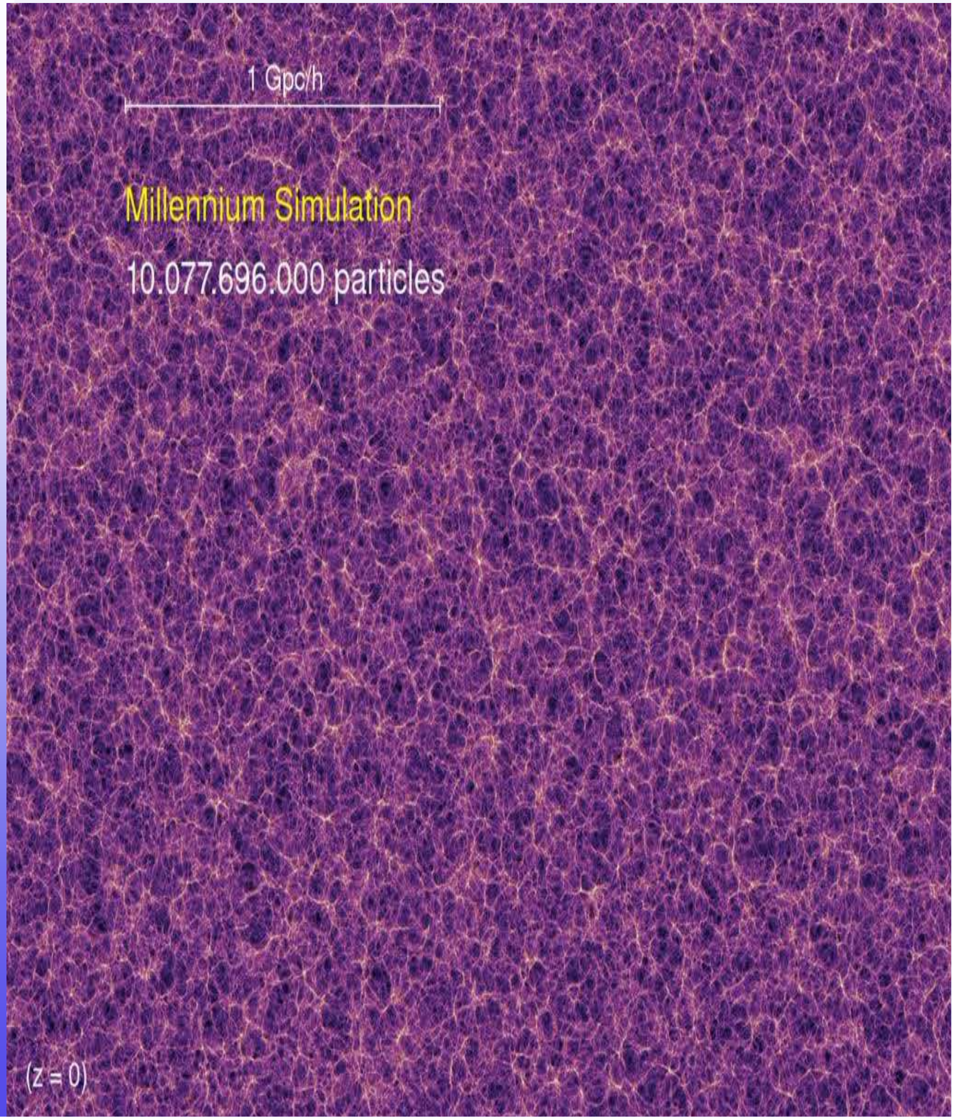

Dark matter distribution

1. **cosmological approach:** **Cold Dark Matter halos achieve the equilibrium density profile** ***(Navarro, Frenk & White, 1996; Moore, Governato, Quinn, Stadel & Lake, 1998):***

cuspy:

$$\rho_{NFW}(r) = \frac{\rho_0}{(r/r_s)(1+r/r_s)^2}$$

$$\rho_{M05}(r) = \frac{\rho_0}{(r/r_s)^{\gamma}[1+(r/r_s)^{3-\gamma}]}, \quad \gamma \cong 1.2$$

2. **'concordance' approach:** **it accounts for the observational evidence at inner radii and converges to the NFW profile at outer radii** ***(Salucci & Burkert, 2000):***

core:

$$\rho_{Burkert}(r) = \frac{\rho_0}{(1+r/r_s)(1+(r/r_s)^2)}$$

3. **empirical approach:** **the simplest halo *velocity* profile that, in combination with the stellar disk, reproduces the Universal Rotation Curve of Spirals** ***(Persic, Salucci & Stel, 1996)***

Dark matter concentration

1. There is a strong correlation between c_{vir} and M_{vir}, with larger concentrations found in lighter halos.

2. Toy models:

☆ Bullock & al., 2001:

$z_{collapse}$ depends only on power spectrum amplitude

$$c_{vir}(M,z) = K\frac{1+z_{collapse}(M_{vir})}{1+z}$$

☆ Eke, Navarro & Steimetz, 2001:

$z_{collapse}$ depends on both amplitude and slope of power spectrum

$$c_{vir}(M,z) = \left(\frac{\Delta_{vir}(z_{collapse})\Omega_m(z)}{\Delta_{vir}(z)\Omega_m(z_{collapse})}\right)^{1/3}\left(\frac{1+z_{collapse}(M_{vir})}{1+z}\right)$$

Dark matter concentration

Predictions versus numerical simulations:

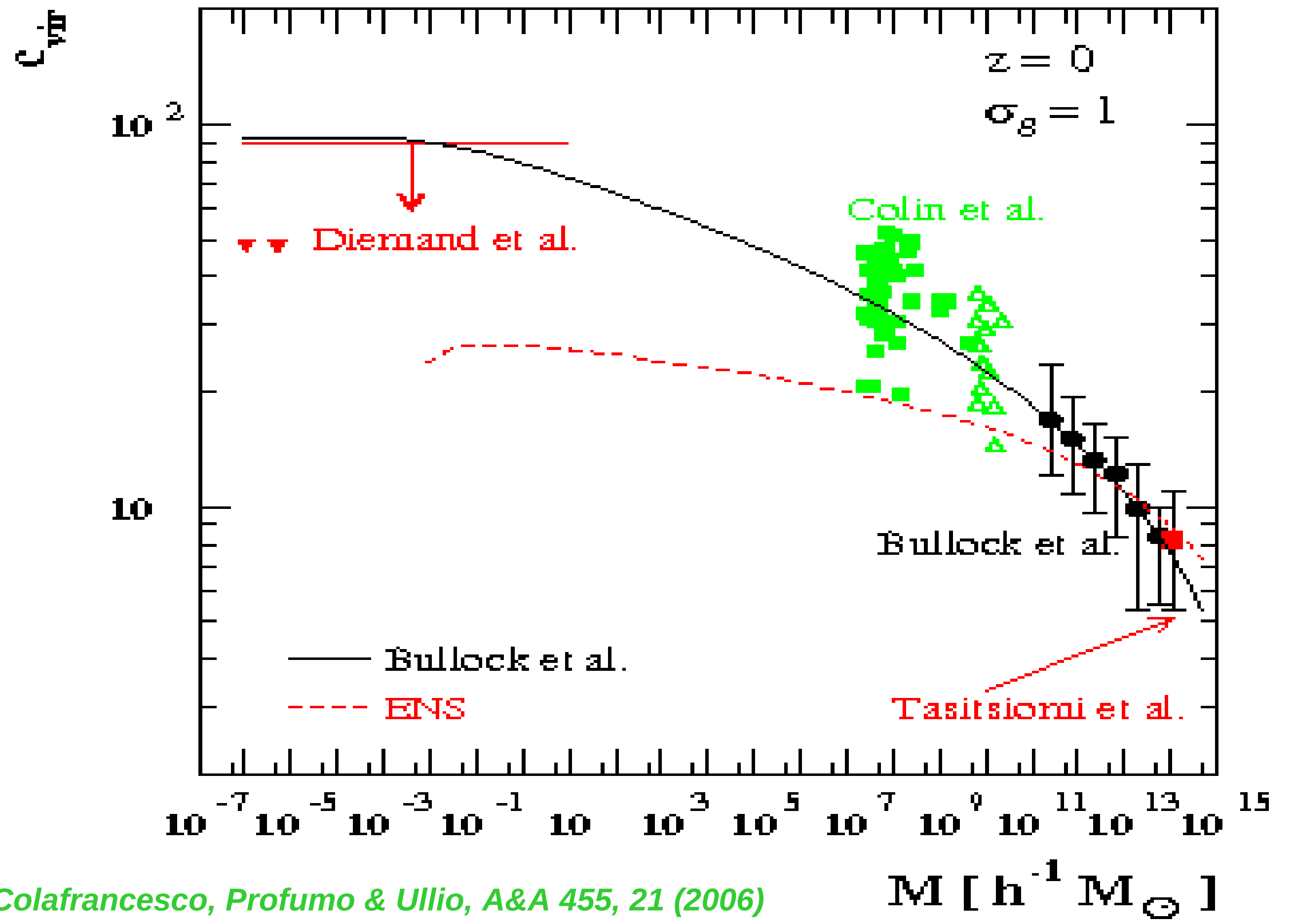

(Colafrancesco, Profumo & Ullio, A&A 455, 21 (2006))

Dynamical evolution

Tidal stripping: **the global tides from host halos strip the outer part of subhalos, resulting either in total subhalo disruption or in significant subhalo mass loss.**

Dynamical friction: **since subhalos reside in very dense environments within the host halos, this effect also plays an important role in driving the subhalo dynamical evolution. It causes the orbital decay of the subhalos, making them more susceptible to strong tidal forces.**

Dynamical evolution

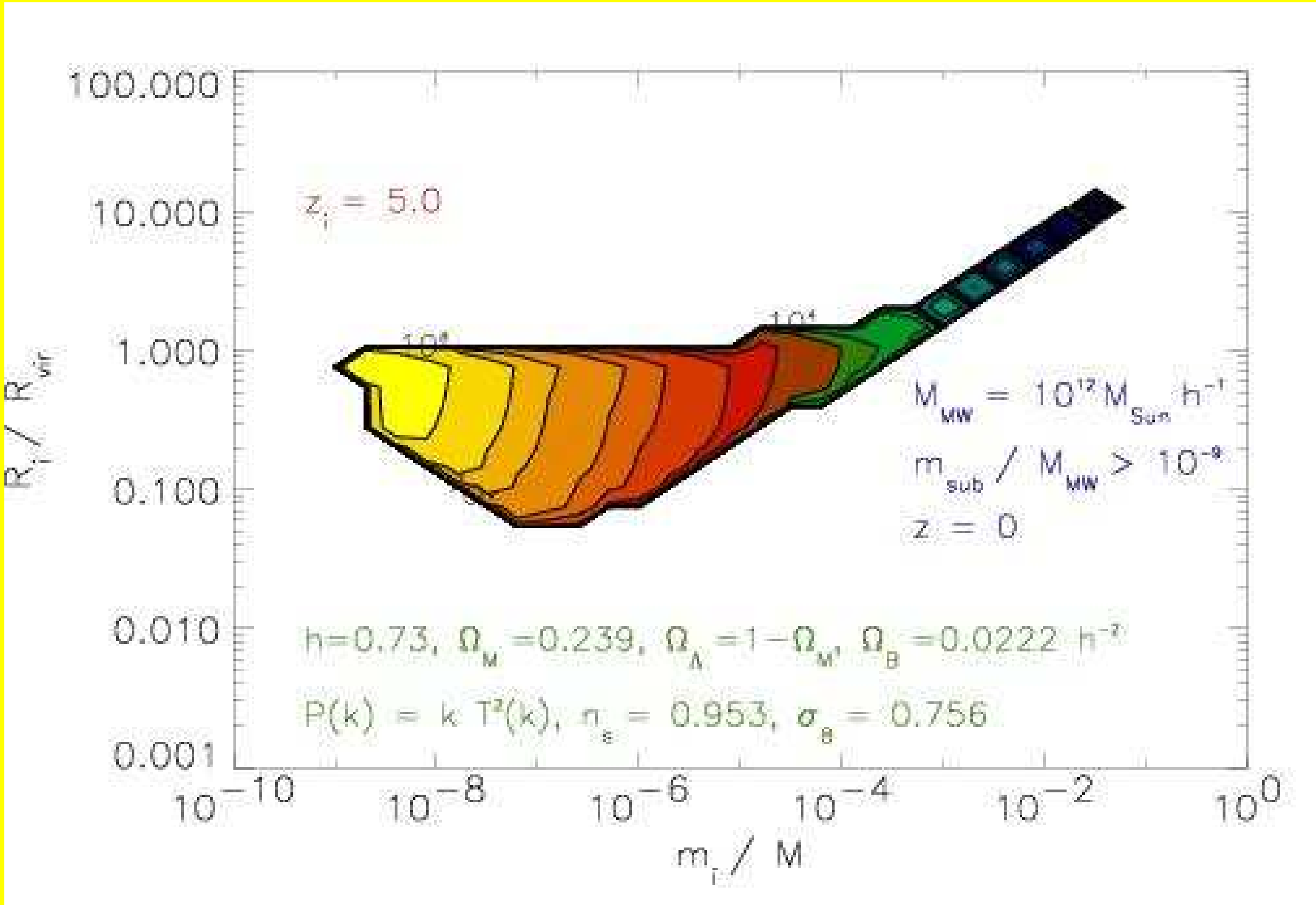

Dynamical evolution

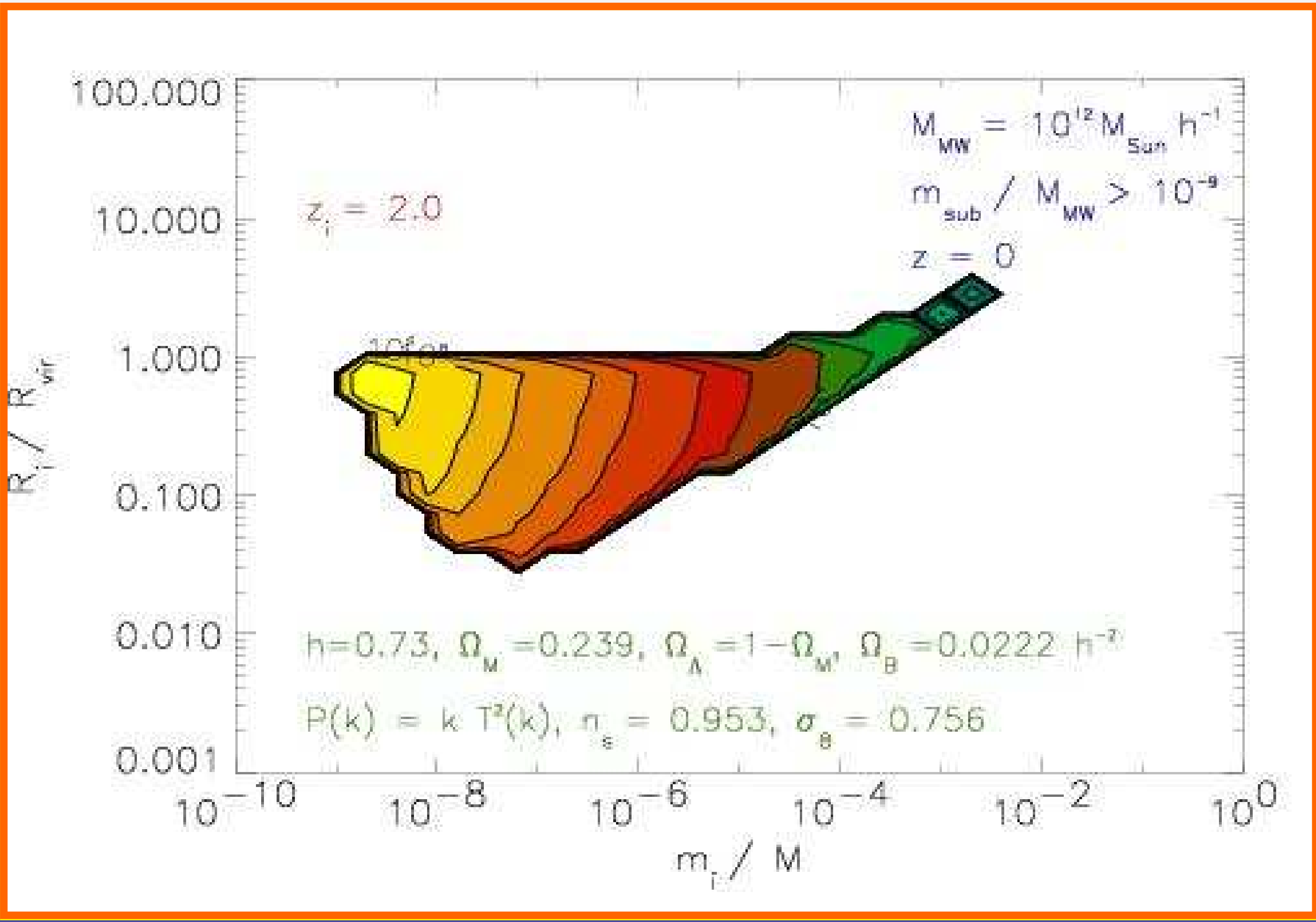

Dynamical evolution

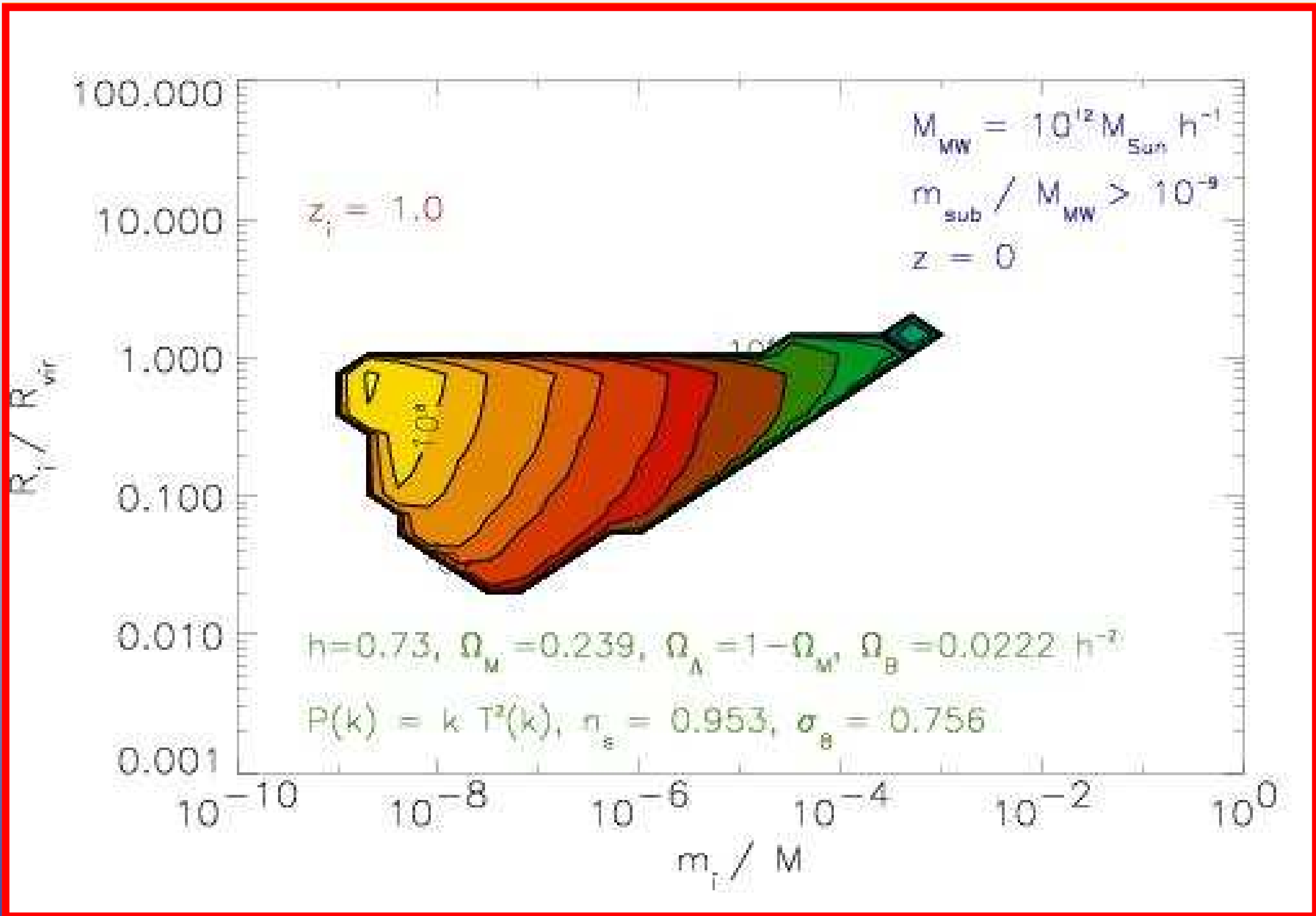

Dynamical evolution

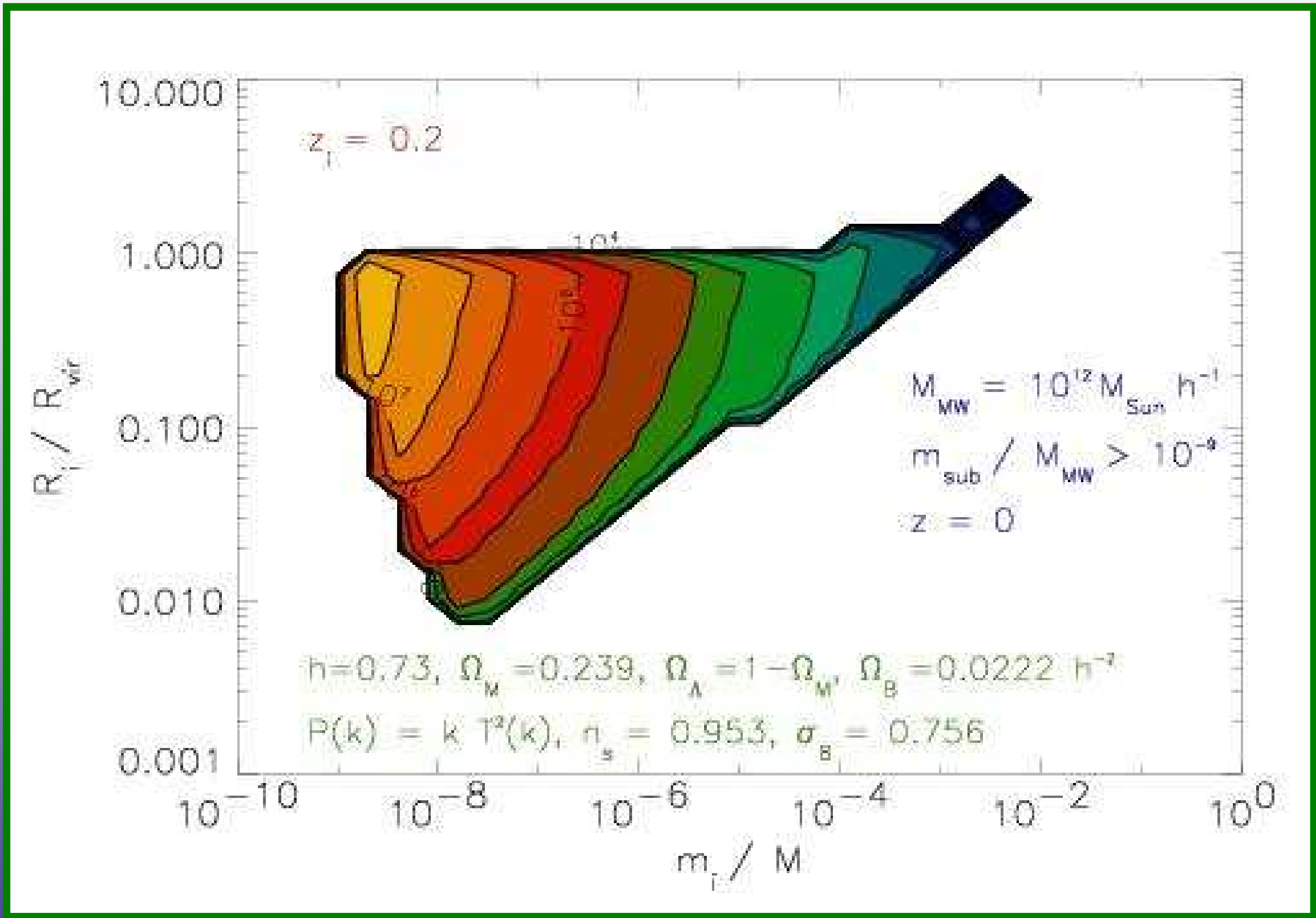

Dynamical evolution

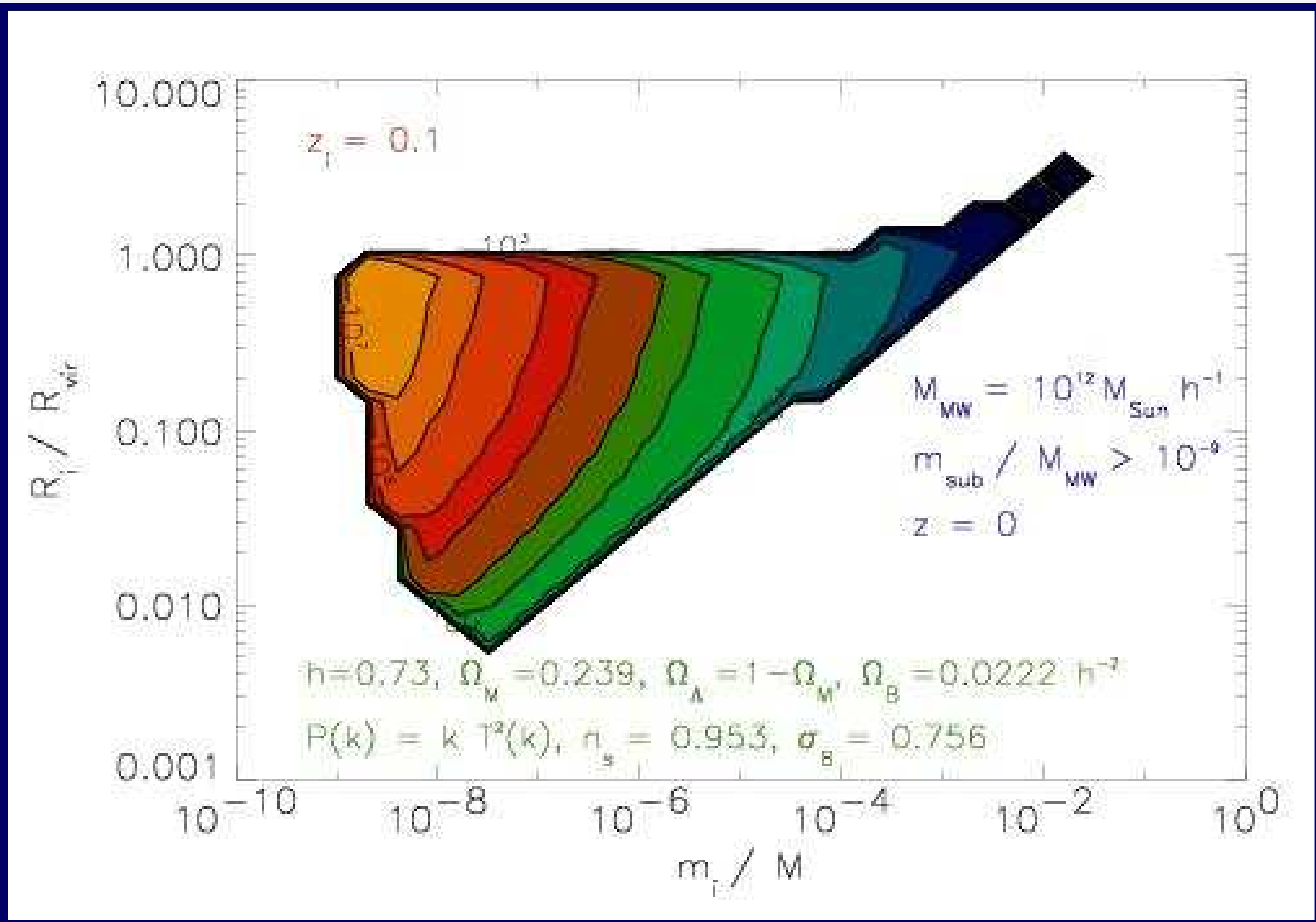

Baryonic component

- The predicted high central density of ΛCDM halos appears to be inconsistent with the observed rotation curves of galaxies.
- <u>Self-treatment of baryons and DM components:</u>

$$M_b(<r) = m_{BH} + 4\pi \int_0^r \rho_b r^2 dr$$

(Klypin, Zhao & Sommerville, 2001 for details)

$$\rho_b = \rho_{nucleus} + \rho_{bulge/bar} + \rho_{disk}$$

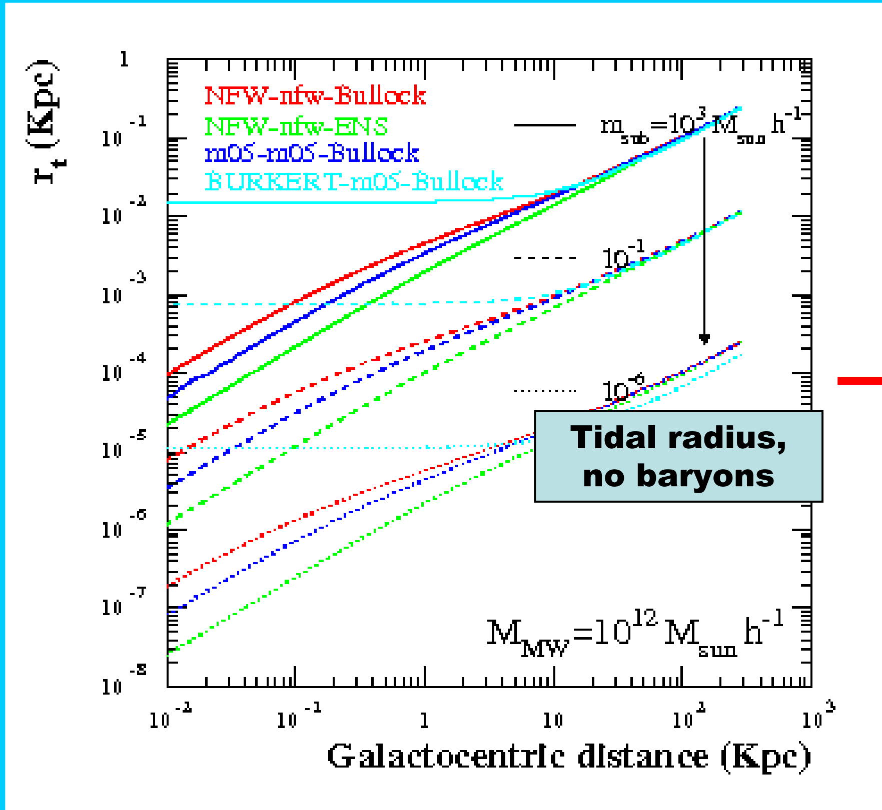

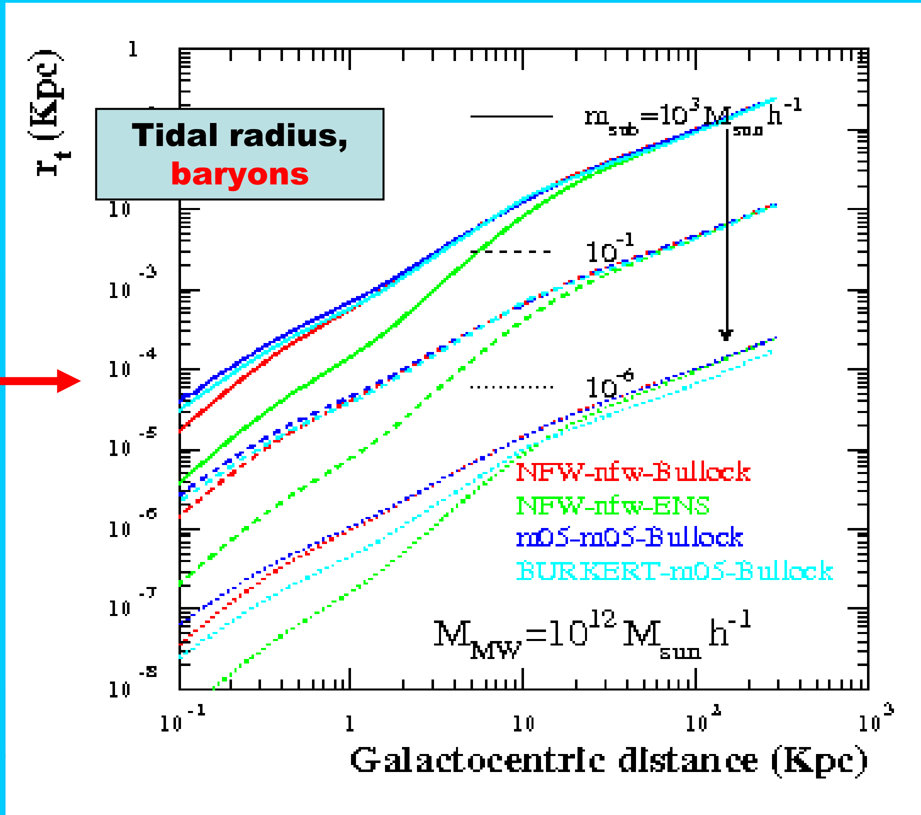

The subhalo spatial mass function

- ♣ **Press & Schechter** formalism → **extended** Press & Schechter → include **spatial correletions** *(Lee, 2004; Oguri & Lee, 2004)*
- ♣ **formation epoch** distribution *(Kitayama & Suto, 1996)*
- ♣ comparison with **numerical simulations** *(De Lucia, 2004)*

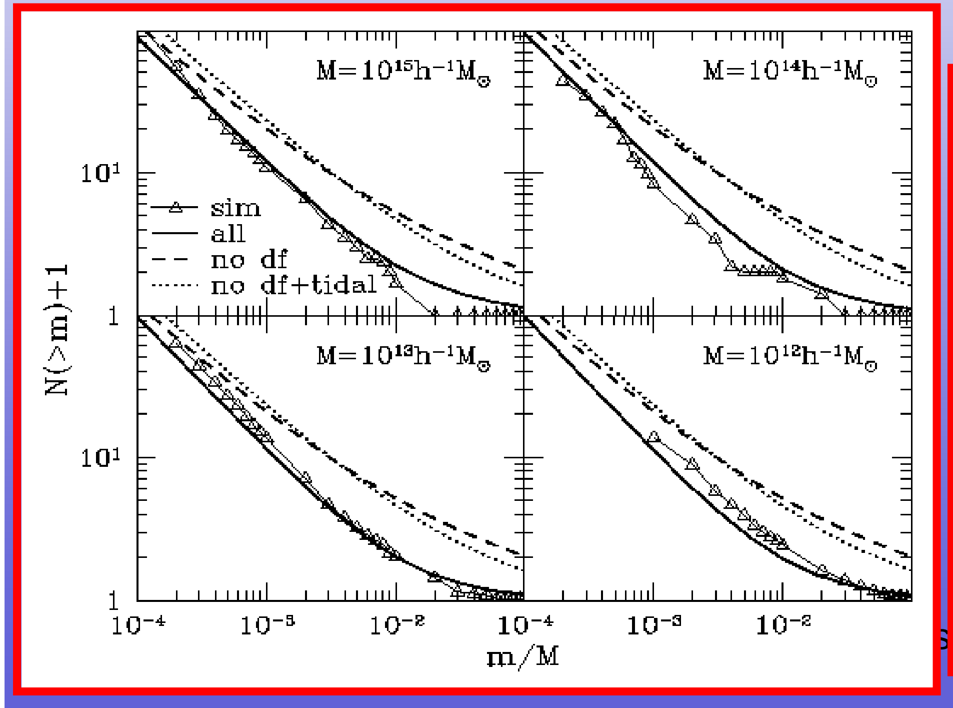

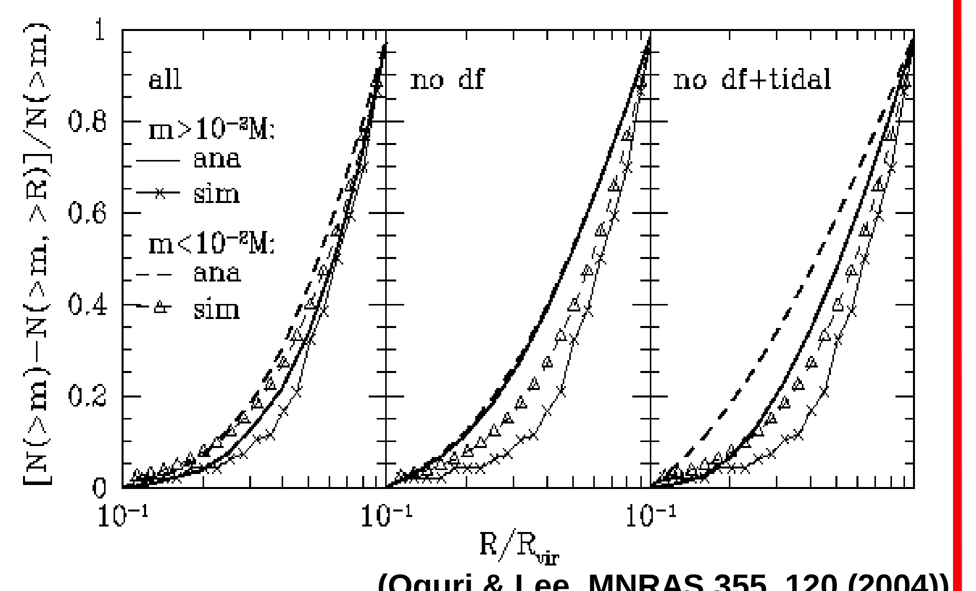

(Oguri & Lee, MNRAS.355, 120 (2004))

Neutralino Dark Matter

From new WMAP and other cosmological data:

(Spergel & al., arXiv:astro-ph/0603449 (2006))

$$\Omega_{TOT} = 1, \quad \Omega_M h^2 = 0.127^{+0.07}_{-0.013}, \quad \Omega_B h^2 = 0.0223^{+0.0007}_{-0.0009}$$

$$h = 0.73 \pm 0.3$$

CDM Relic Density:

$$0.081 < \Omega_\chi h^2 < 0.123$$

The lightest neutralino ($\chi_o^1 = \chi$ = LSP) of MSSM
is massive (some 10 GeV – some TeV),
stable, neutral and cold
(interacts weakly with ordinary matter)

Supersymmetric models

MSSM models:

their action has **seven free parameters:**

$$m_A,\ m_0,\ M_2,\ sign(\mu),\ \tan\beta,\ A_0,\ A_t$$

LEP limits: Mass of sparticles > E_{beam}

$\tan\beta > 2.5$, $m_h > 114.4\ GeV$, $m_{\chi^\pm} > 103.5\ GeV$, $m_{\chi^o} > 58.6\ GeV$

mSUGRA models:

- Unify Higgs and scalar sector at the GUT scale
- Unify all trilinear couplings at the GUT scale
- Break radiatively the electroweak symmetry
- Under the assumption of universality at the GUT scale,

their action has *five free parameters:*

$$m_0,\ M_{1/2},\ sign(\mu),\ A_0,\ \tan\beta$$

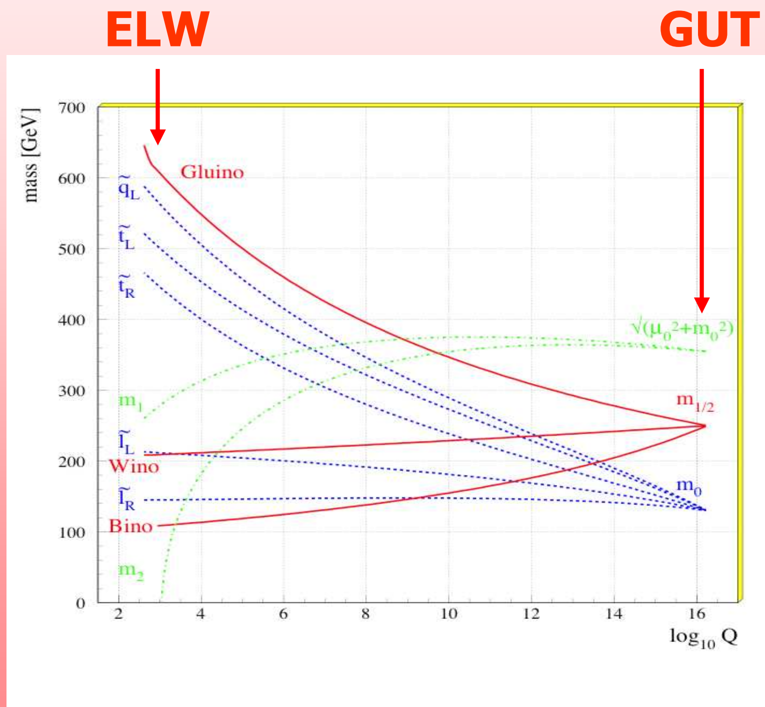

LEP limits: Mass of sparticles > E_{beam}

$\tan\beta > 2.5$, $m_h > 114.4\ GeV$, $m_{\chi^\pm} > 103.5\ GeV$, $m_{\chi^0} > 58.6\ GeV$

mSUGRA models:

- Unify Higgs and scalar sector at the GUT scale
- Unify all trilinear couplings at the GUT scale
- Break radiatively the electroweak symmetry
- Under the assumption of universality at the GUT scale,

their action has *five free parameters:*

$$m_0,\ M_{1/2},\ sign(\mu),\ A_0,\ \tan\beta$$

LEP limits: Mass of sparticles > E_{beam}

$$\tan\beta > 2.5,\quad m_h > 114.4\ GeV,\quad m_{\chi\pm} > 103.5\ GeV,\quad m_{\chi_0} > 58.6\ GeV$$

mSUGRA regions:

- **Slepton coannihilations region (bulk region):**

  $A_0 = 0;\quad m_0 \lesssim m_{1/2}$

- **Chargino coannihilations region (focus point region):**

  $m_0 >> m_{1/2}$

- **Stop coannihilations region:**

  Larger A_0

Neutralino detectability

- **Direct searches;**
- **Collider experiments;**
- **Indirect searches:**
  - γ rays (continuum, lines)
  - synchrotron and inverse Compton emission from the charged annihilation products
  - cosmic antiprotons, positrons
  - neutrinos

MULTIWAVELENGHT APPROACH

Signals enhancement from substructures

$N_{pairs}(r)=\rho^2(r) <\sigma v>/m_\chi^2$
$\rho(r_0)=0.3$ GeV cm^{-3}
$r_0=8.0$ Kpc

number density of N_{pairs} due to subhalos as a function of Galactocentric radius

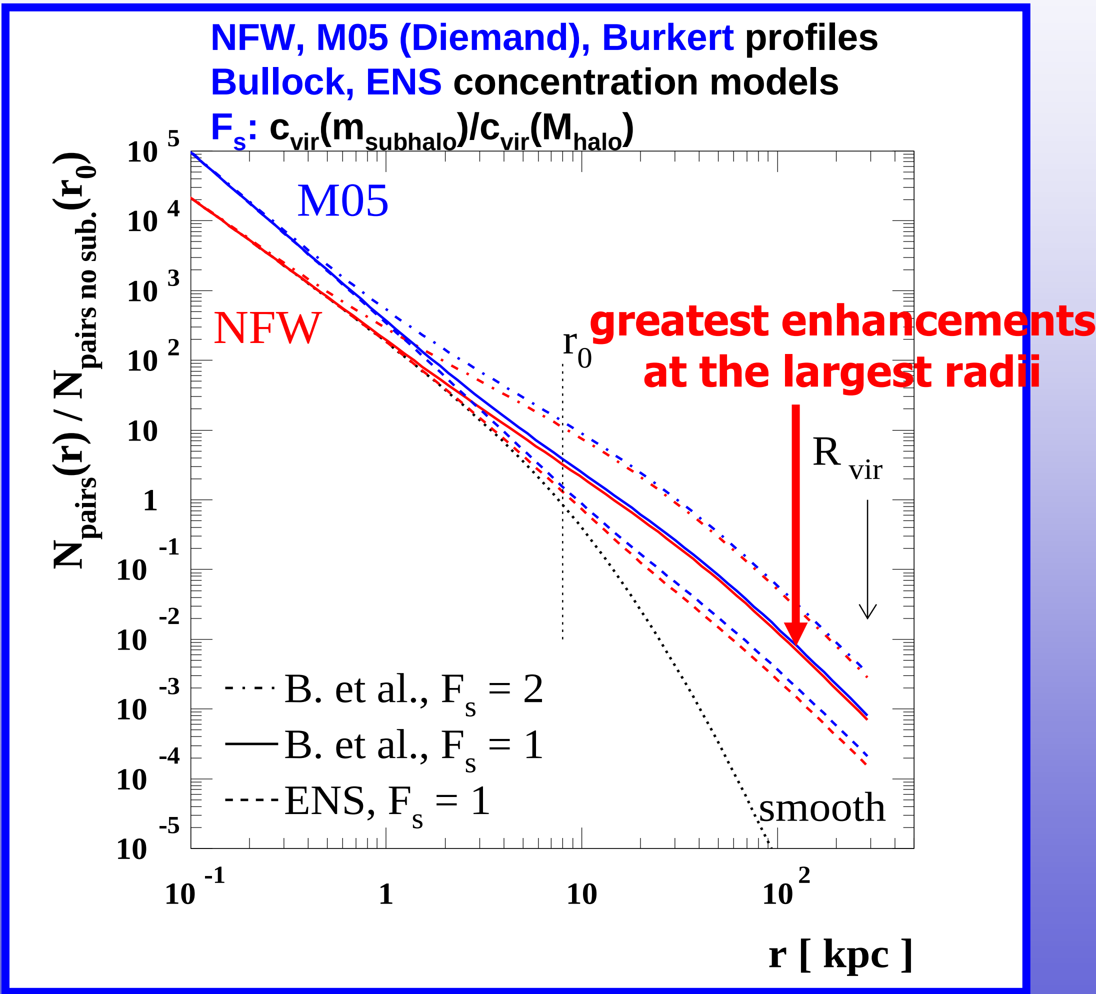

Signals enhancement from substructures

$N_{pairs}(r)=\rho^2(r) <\sigma v>/m_\chi^2$
$\rho(r_0)=0.3$ GeV cm^{-3}
$r_0=8.0$ Kpc

subhalos-related enhancement of N_{pairs} versus the ratio of the concentration parameter of subhalos and halos of equal mass

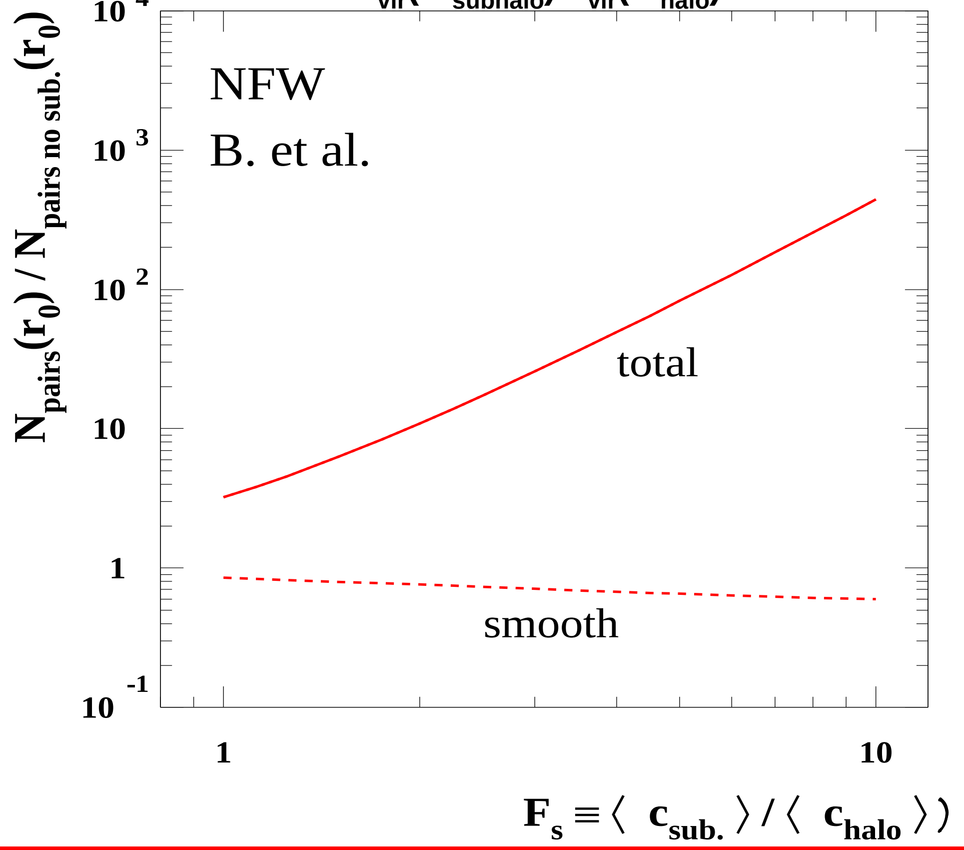

Gamma-ray fluxes

Smooth component:

SUSY MODELS:

- MSSM, mSUGRA
- WMAP constraints on ‹σv›
- Accelerator constraints

$$< J(l,b) >_{(\Delta\Omega)} = \int_{los} dl\, \rho^2(r)$$

$$F_\gamma(E > E_{th}) \propto \frac{N_\gamma \langle \sigma v \rangle}{\Delta\Omega \cdot 2m_\chi^2} \cdot < J(l,b) >_{(\Delta\Omega)}$$

ΛCDM COSMOLOGY:

- Observations constraints
- N-body simulations

Gamma-ray fluxes

Subhalo component:

$$< J(l,b) >_{(\Delta\Omega)} = \int_{los} dl \int_{z_i}^{z_f} \frac{dp}{dz} dz \int_{m_{\min}}^{m_{\max}} dm \frac{d^2 N}{dm\, d^3 r} \int_0^{r_{cl}} dr\, 4\pi r^2 \rho^2{}_{cl}(m,r,z)$$

SUSY MODELS:

- MSSM, mSUGRA
- WMAP constraints on ‹σv›
- Accelerator constraints

$$F_\gamma(E > E_{th}) \propto \frac{N_\gamma \langle \sigma v \rangle}{\Delta\Omega \cdot 2m_\chi^2} \cdot < J(l,b) >_{(\Delta\Omega)}$$

ΛCDM COSMOLOGY:

- Observations constraints
- N-body simulations

Gamma-ray signal

Two WIMP models with given annihilation rate, dominant annihilation final state into $b\bar{b}$ and mass M_χ = 50 GeV or 100 GeV;

NFW universal shape profile;

Fs = 2, as extrapolated with the Bullock & al. prescription;

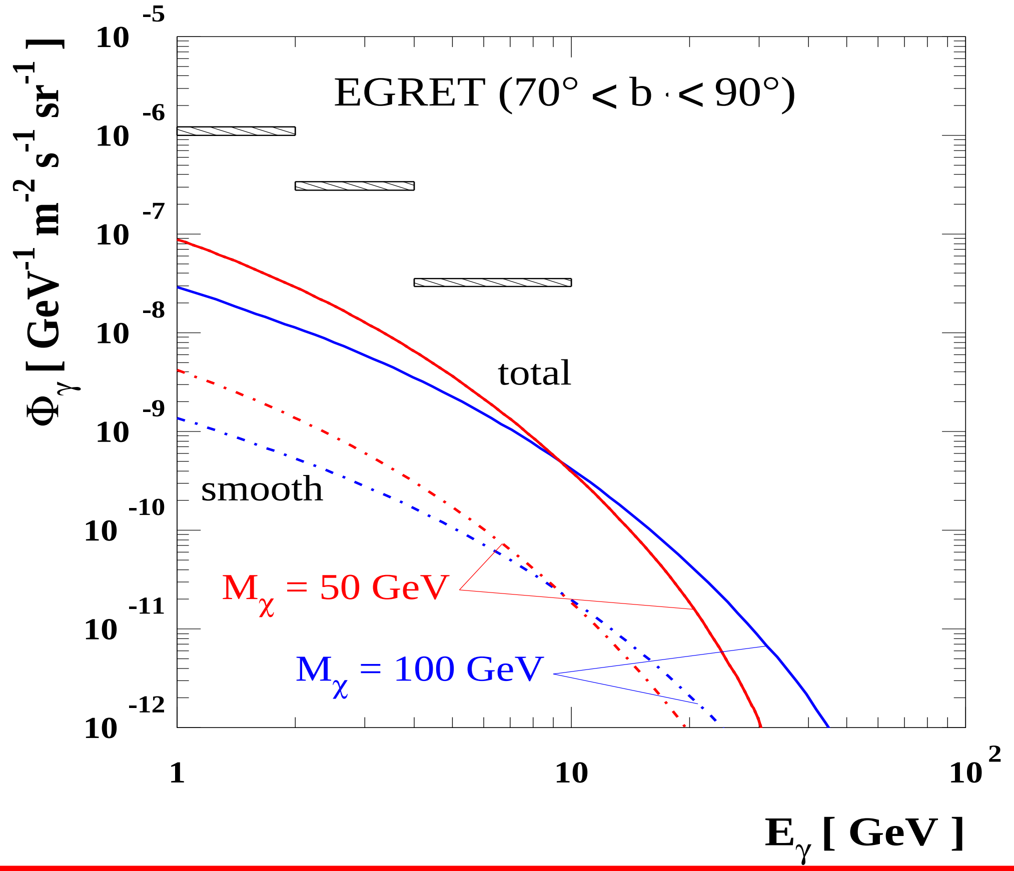

Fluxes from antiprotons and positrons

Source function:

$$Q_{\bar{p},e^+}(E,\vec{x}) = \frac{1}{2}(\sigma_{ann}v)\left(\frac{\rho_\chi(\vec{x})}{m_\chi}\right)^2 \sum_f B_f \frac{dN_f}{dE}$$

Plug into diffusion equaton:

(Bergström & al., ApJ 526, 215B (1999))

$$\frac{\partial}{\partial t}N_{\bar{p}}(E,\vec{x}) = \nabla\left[D(R,\vec{x})\nabla N_{\bar{p}}(E,\vec{x})\right] - \nabla\cdot(\vec{u}(\vec{x})N_{\bar{p}}(E,\vec{x})) - p(E,\vec{x})N_{\bar{p}}(E,\vec{x}) + Q_{\bar{p}}(E,\vec{x}) = 0$$

$$\frac{\partial}{\partial t}\frac{dn_{e^+}}{dE} = \nabla\left[D(E,\vec{x})\nabla\frac{dn_{e^+}}{dE}\right] + \frac{\partial}{\partial E}\left[b_{e^+}(E,\vec{x})\frac{dn_{e^+}}{dE}\right] + Q_{e^+}(E,\vec{x})$$

(Baltz & Edsjö, Ph.Rv.D. 59b 3511B (1999))

$$\Phi_{\bar{p},e^+}(E_{\bar{p},e^+})$$

Antiproton signal

Two WIMP models with given annihilation rate, dominant annihilation final state into $b\bar{b}$ and mass M_χ = 50 GeV or 100 GeV;

NFW universal shape profile;

Fs = 2, as extrapolated with the Bullock & al. prescription;

all fluxes displayed are solar modulated and data taken at the corresponding phase of the solar cycle are plotted.

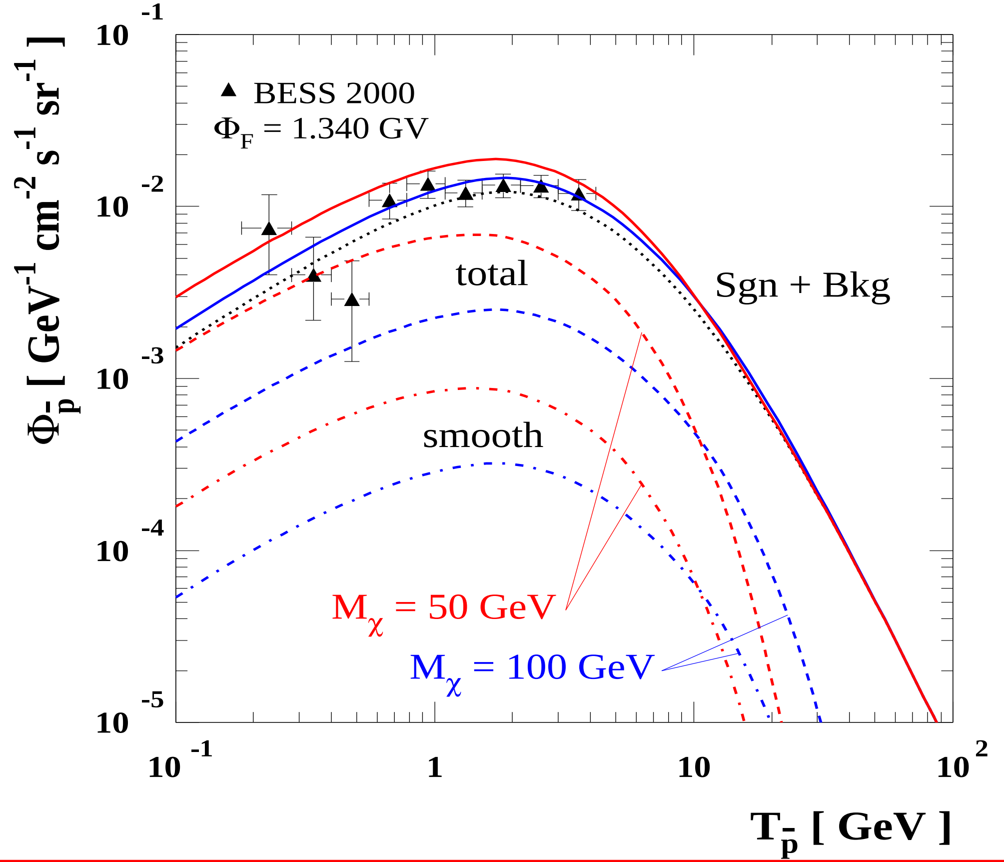

Positron signal

Two WIMP models with given annihilation rate, dominant annihilation final state into $b\bar{b}$ and mass M_χ = 50 GeV or 100 GeV;

NFW universal shape profile;

Fs = 2, as extrapolated with the Bullock & al. prescription;

all fluxes displayed are solar modulated and data taken at the corresponding phase of the solar cycle are plotted.

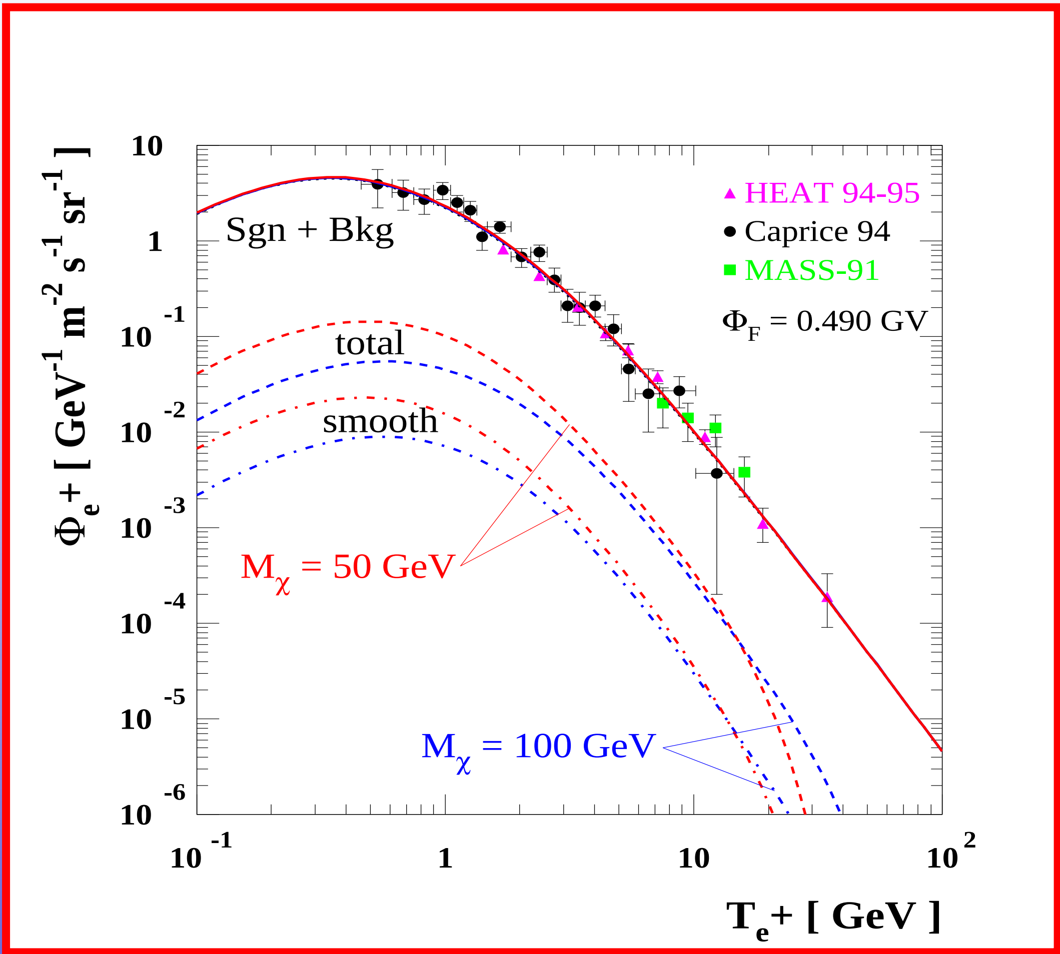

Discussion and predictions

Upper limits on the annihilation rate <σv>

(3σ limits)

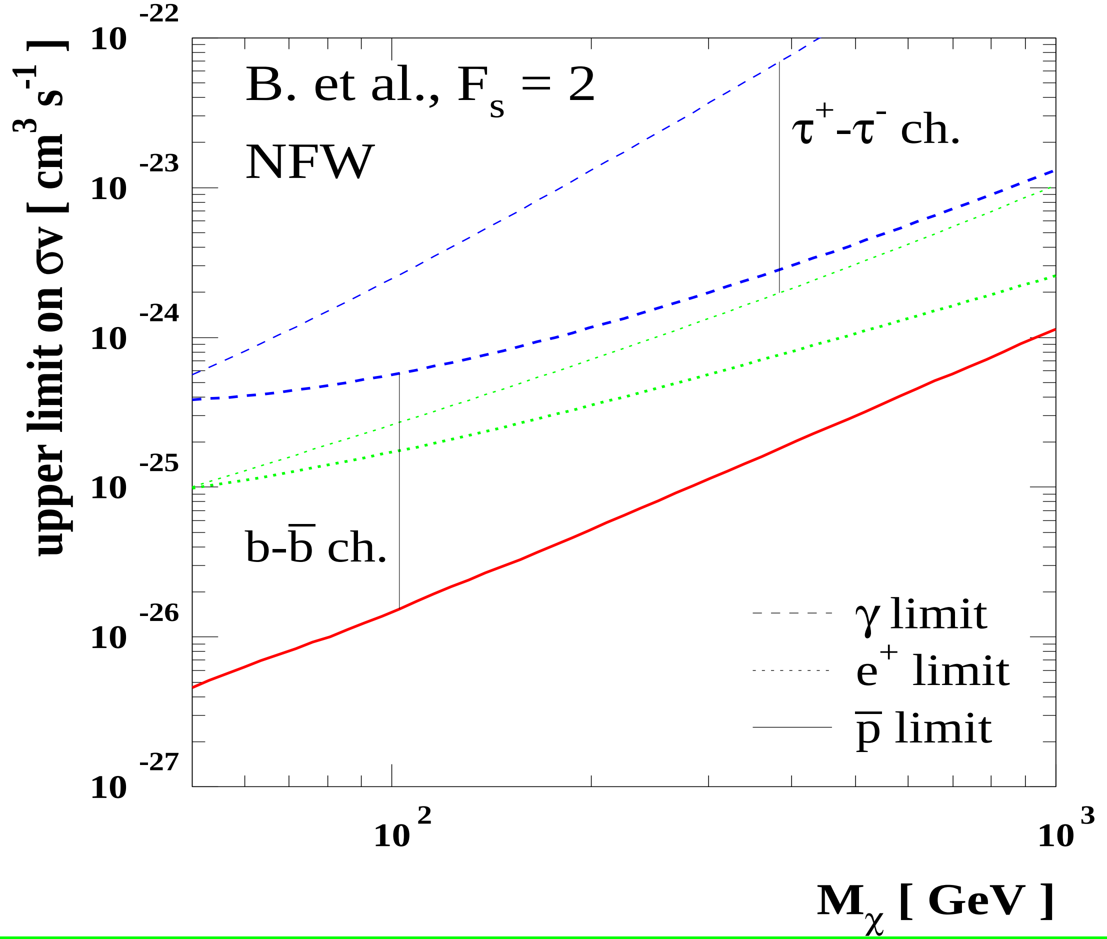

Discussion and predictions

Enhancement of the antiproton, positron and gamma-ray flux;

NFW universal profile;

in subhalos: concentration parameter is larger by factor Fs than in progenitor halos of same mass (Bullock & al.).

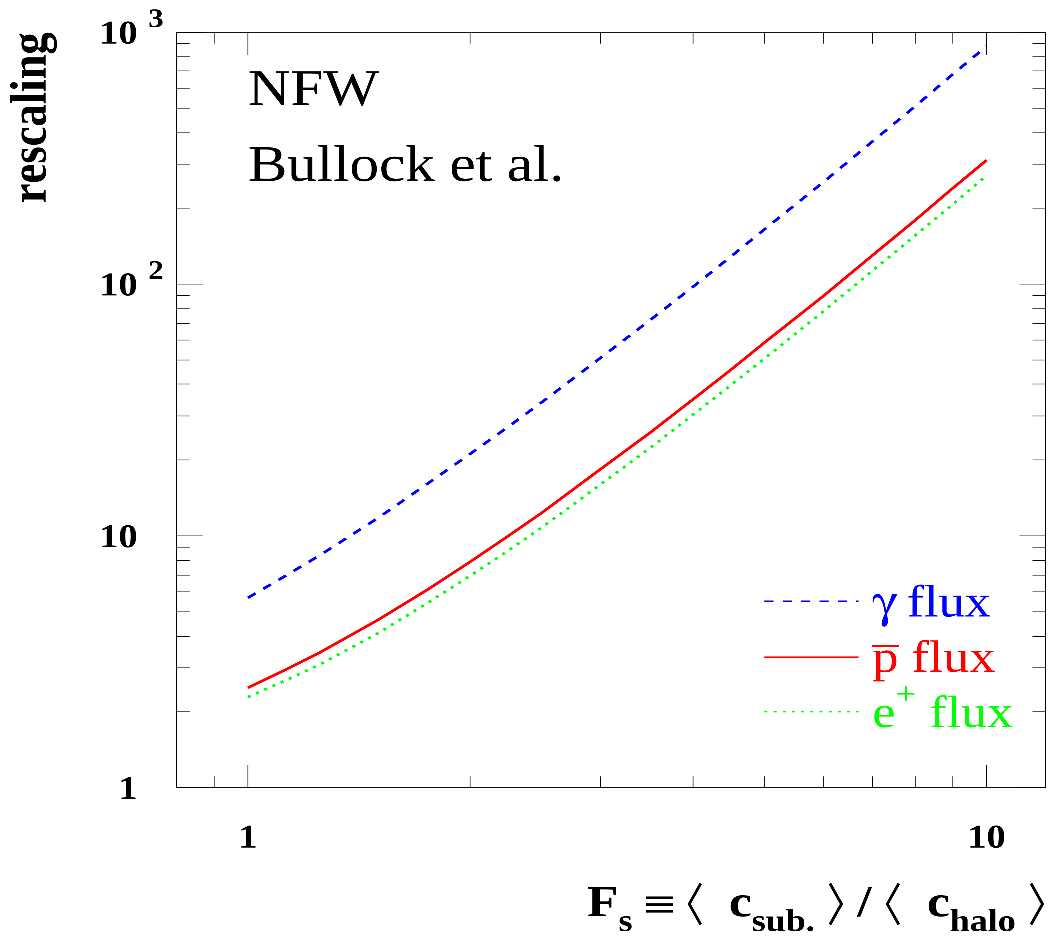

EGRET unidentified sources as dark matter clumps?

Selection over the Third EGRET Catalog:

1. 'A' (AGN), 'a' (possible AGN), 'S' (SF): filtered out
2. $|b| \geq 15°$
3. Steady source

3EG_1835+5918

1. $(l,b) = (88.74°, 25.07°)$
2. spectral index $\gamma = 1.69$

Best SUSY model:

1. $b^{-}b$ channel
2. $m_\chi = 46.17$ GeV c^{-2}
3. $< \sigma v > = 6.38 \cdot 10^{-26}$ cm^3 s^{-1}
4. $\Omega_\chi h^2 = 0.048$

Is there any chance to identify a single DM clump?

$$\frac{\int_0^{r_t(R_f(d),m_i^*)} \rho^2(r,m_i^*)4\pi r^2\,dr}{d^2} - \varepsilon_{\min} = 0$$

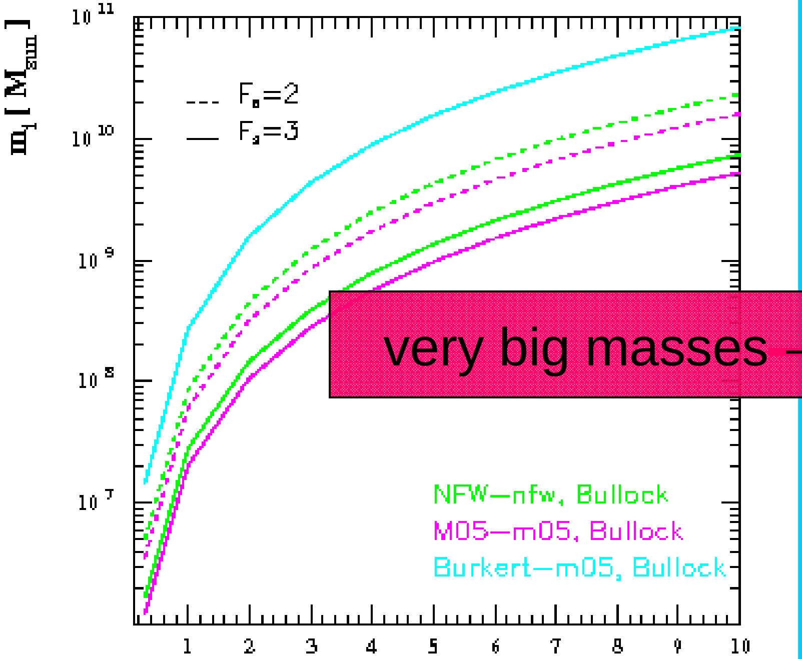

initial clump mass

very big masses → very low probability

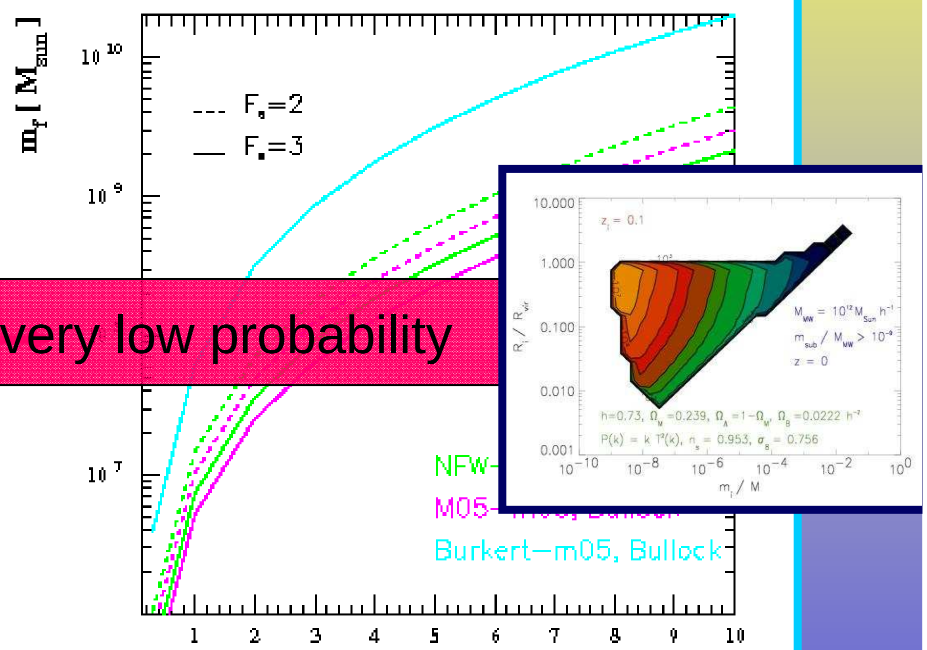

final clump mass

The MAGIC Telescope

International collaboration among 16 Institutes in more than 10 Countries, involving about 150 members (Barcelona IFAE, Barcelona UAB, Barcelona UB, Crimean Observatory, U.C. Davis, U. Lodz, UCM Madrid, MPI Munich, INFN/ U. Padua, INFN/ U. Siena, U. Humboldt Berlin, Tuorla Observatory, Yerevan Phys. Institute, INFN/U. Udine, U. Würzburg, ETH Zürich, INR Sofia, Univ. Dortmund)

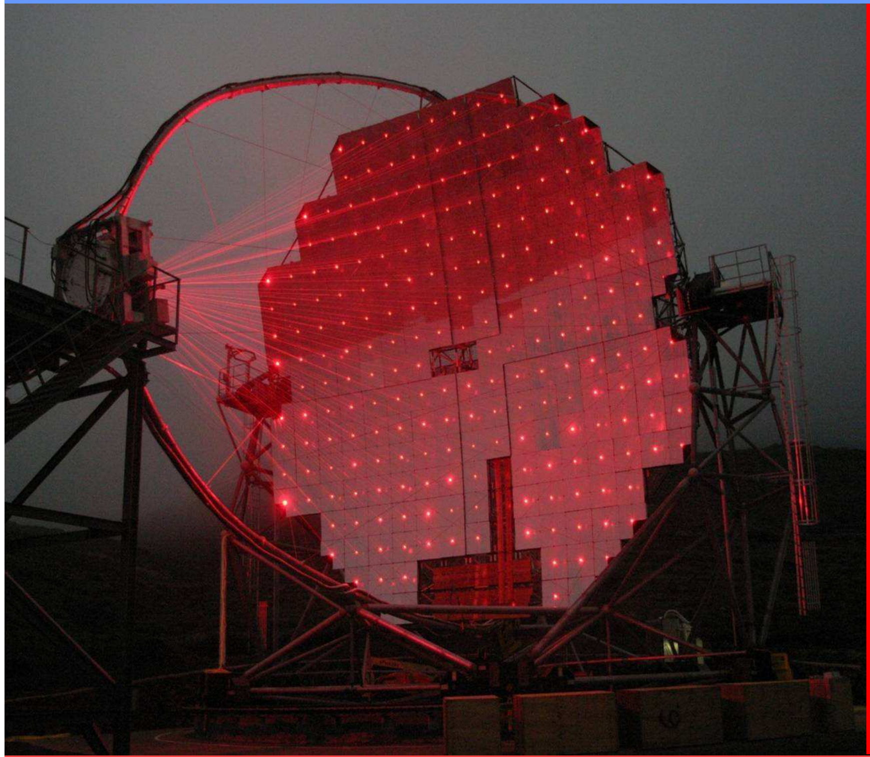

- MAGIC is a **Cherenkov Telescope (IACT)** at the **Roque de los Muchachos** Observatory**,** La Palma, Canary Islands (Spain) at **28.8°N;**
- **energetic range: 50 GeV - 50 TeV;**
- **mirror diameter**: **17 m Ø** $\Rightarrow$ **low energetic** threshold;
- **camera FOV: 3.5° Ø;**
- **angular resolution: ~ 0.1° (TeV),** allowing the determination of the point-source **position within 2';**
- **energetic resolution: 20-30%;**
- **sensitivity: 2.5%** of the **Crab Nebula** within **5σ in 50 h;**
- **rapid repositioning: (< 40 s on average)** for γ-ray bursts observations;
- **moon observation** possible $\Rightarrow$ 50% extra-observation time

The MAGIC Telescope

International collaboration among 16 Institutes in more than 10 Countries, involving about 150 members **(Barcelona IFAE, Barcelona UAB, Barcelona UB, Crimean Observatory, U.C. Davis, U. Lodz, UCM Madrid, MPI Munich, INFN/ U. Padua, INFN/ U. Siena, U. Humboldt Berlin, Tuorla Observatory, Yerevan Phys. Institute, INFN/U. Udine, U. Würzburg, ETH Zürich, INR Sofia, Univ. Dortmund)**

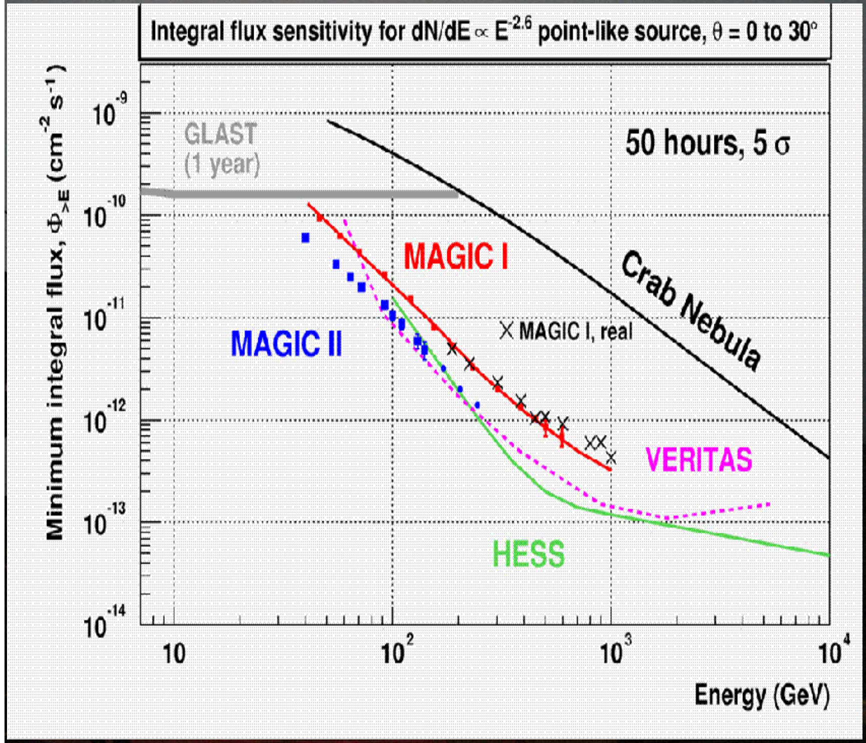

- MAGIC is a **Cherenkov Telescope (IACT)** at the **Roque de los Muchachos** Observatory**,** La Palma, Canary Islands (Spain) at **28.8°N;**
- **energetic range: 50 GeV - 50 TeV;**
- **mirror diameter**: **17 m Ø** ⇒ **low energetic** threshold;
- **camera FOV: 3.5° Ø;**
- **angular resolution: ~ 0.1° (TeV),** allowing the determination of the point-source **position within 2';**
- **energetic resolution: 20-30%;**
- **sensitivity: 2.5%** of the **Crab Nebula** within **5σ in 50 h;**
- **rapid repositioning: (< 40 s on average)** for γ-ray bursts observations;
- **moon observation** possible ⇒ 50% extra-observation time

The MAGIC Telescope

Standard MAGIC data analysis

First run selection:
- correct working of the trigger system
- good atmospheric conditions
- no technical problems
- sufficient quantity of events

Calibration
Image cleaning
Hillas paramaters

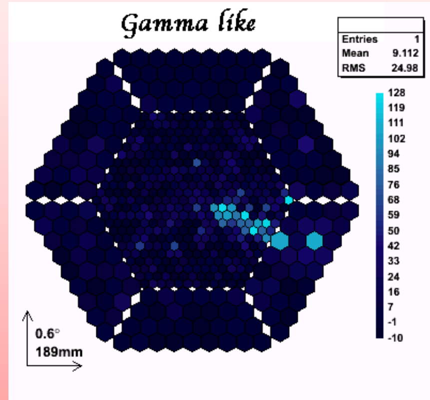

Second run selection:
- high rate
- camera homogeneity
- good quality data

Gamma-hadron separation:
- supercuts
- Random Forests

HADRONNESS

Source position reconstruction:
- source dependent analysis **(α plot)**
- source independent analysis **(DISP method, θ^2 plot)**

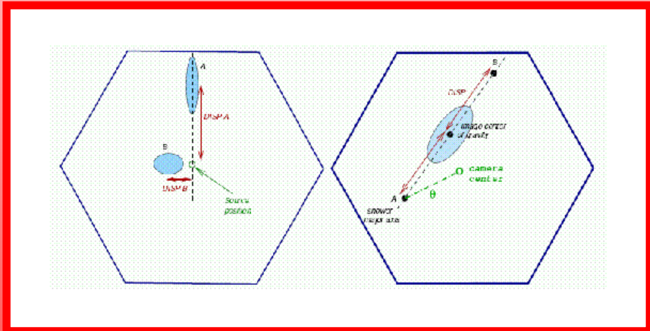

Energy estimation

Signal evaluation:
- significance calculation **(Li & Ma method)**
- flux sensitivity
- upper limits **(5σ)**

The Crab Nebula

Period 25:

2.5 hours **ON** between 3 and 4 January, 2005
2.6 hours **OFF** between 7 and 8 January, 2005

Compatibility of data:

- zenith angle
- event rate
- pedestal RMS
- PSF
- inhomogeneity

Calibration with Spline extractor
Image cleaning: Absolute 10:5

Random Forest training:

- SIZE, WIDTH, LENGHT, CONC, CONC7, M3LONG

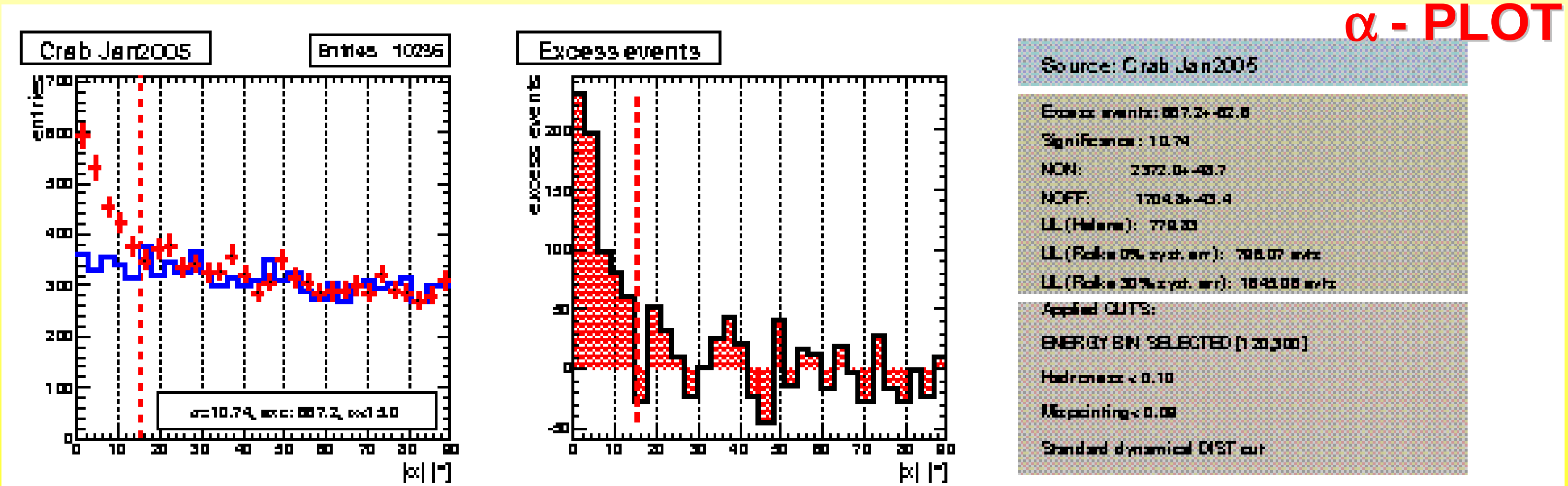

The Crab Nebula

Period 25:

2.5 hours **ON** between 3 and 4 January, 2005
2.6 hours **OFF** between 7 and 8 January, 2005

Compatibility of data:

- zenith angle
- event rate
- pedestal RMS
- PSF
- inhomogeneity

Calibration with Spline extractor
Image cleaning: Absolute 10:5

Random Forest training:

- SIZE, WIDTH, LENGHT, CONC, CONC7, M3LONG

θ^2 PLOT

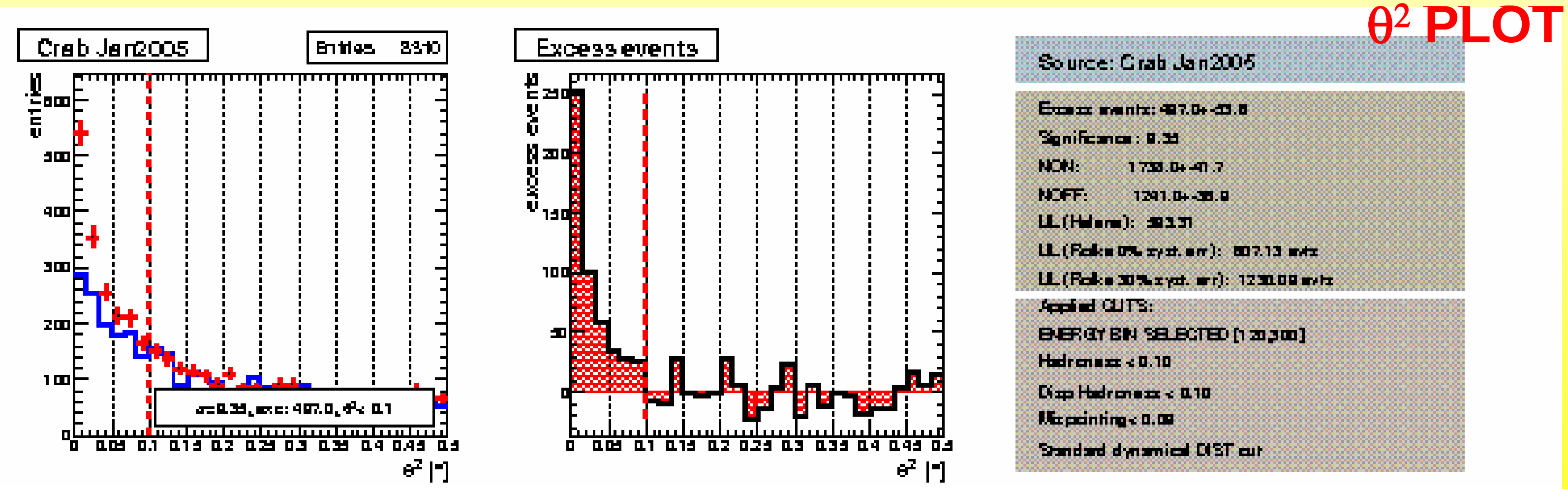

CRAB SKYMAP in ENERGY bins

HADRONNESS cut 0.2

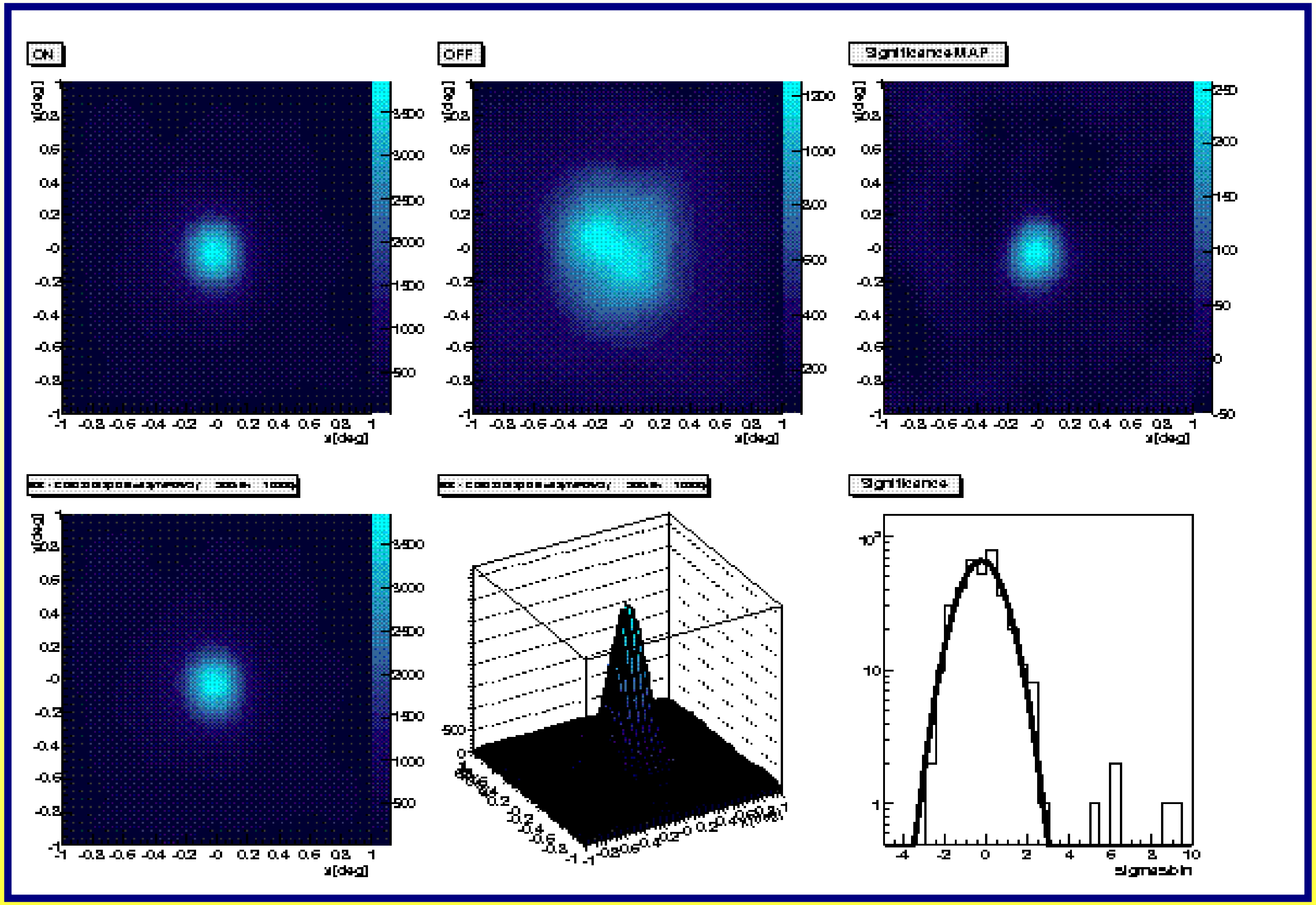

DIFFERENTIAL SPECTRUM OF CRAB

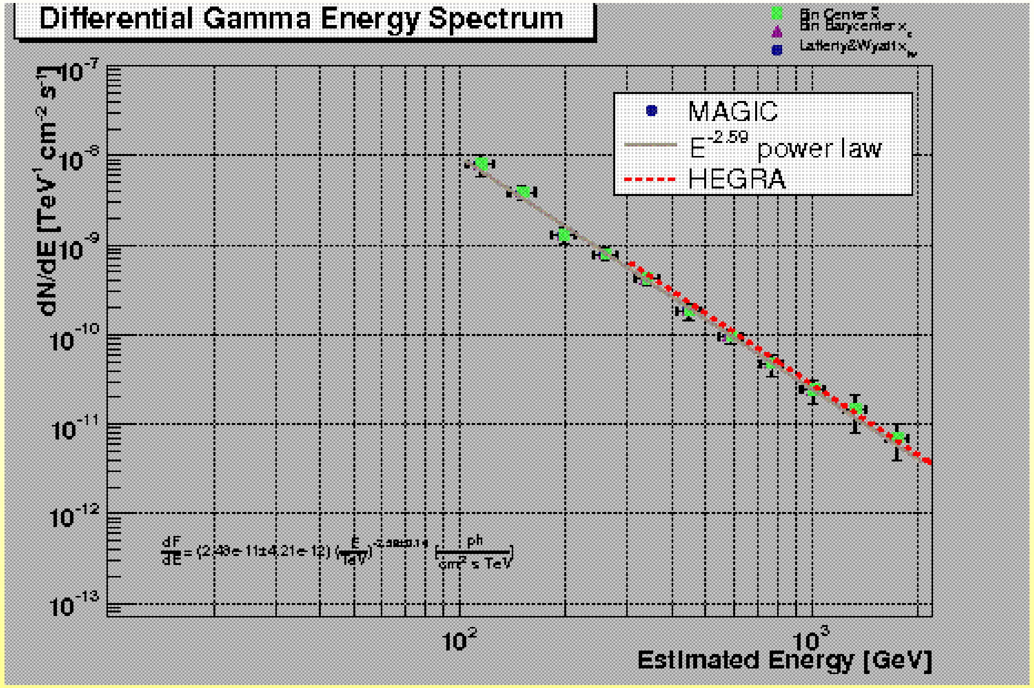

CONCLUSIONS:

1. **significance** is in good agreement with previous MAGIC results;
2. sky map projection confirms **coordinates** of source;
3. differential spectrum: **power law,** in agreement with previous analyses;
4. **energy interval** of this analysis: **100 GeV - 1 TeV.**

3EG_J1835+5918

Between May and June, 2006:
30 hours **ON**
5 hours **OFF**

Calibration with Digital Filter extractor
Image cleaning: Absolute 7:5

Strong camera inhomogeneity:

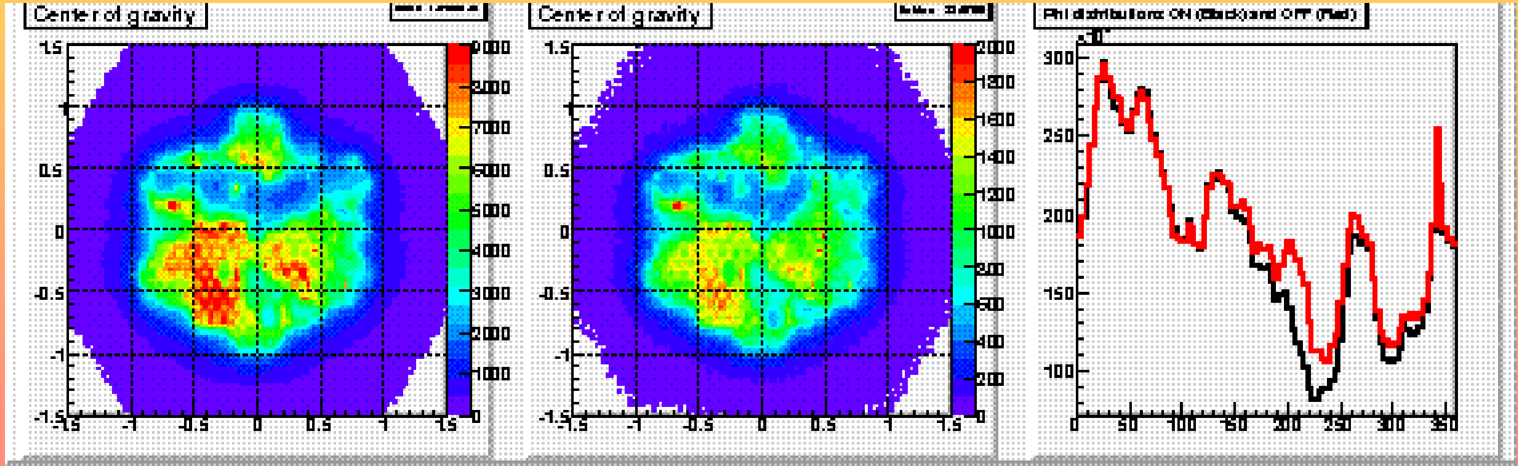

MAGIC Collaboration

3EG_J1835+5918

Between May and June, 2006:
30 hours **ON**
5 hours **OFF**

Calibration with Digital Filter extractor
Image cleaning: Absolute 7:5

Strong camera inhomogeneity:

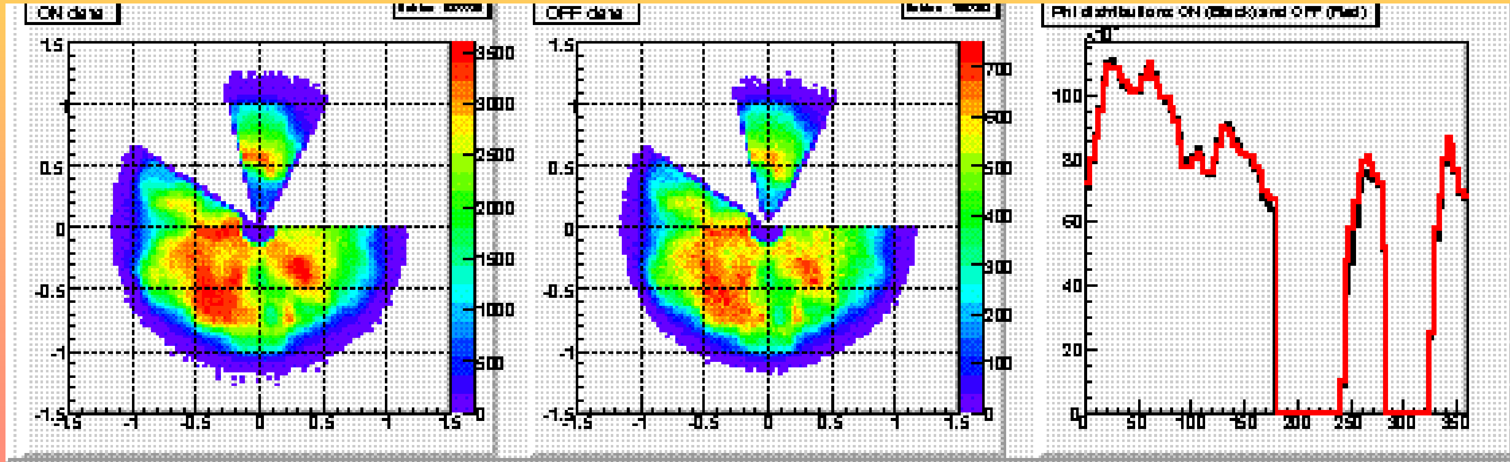

MAGIC Collaboration

HINT OF AN ECCESS: α – PLOT, θ^2 – PLOT (120–300 GeV, 30–36 ZA)

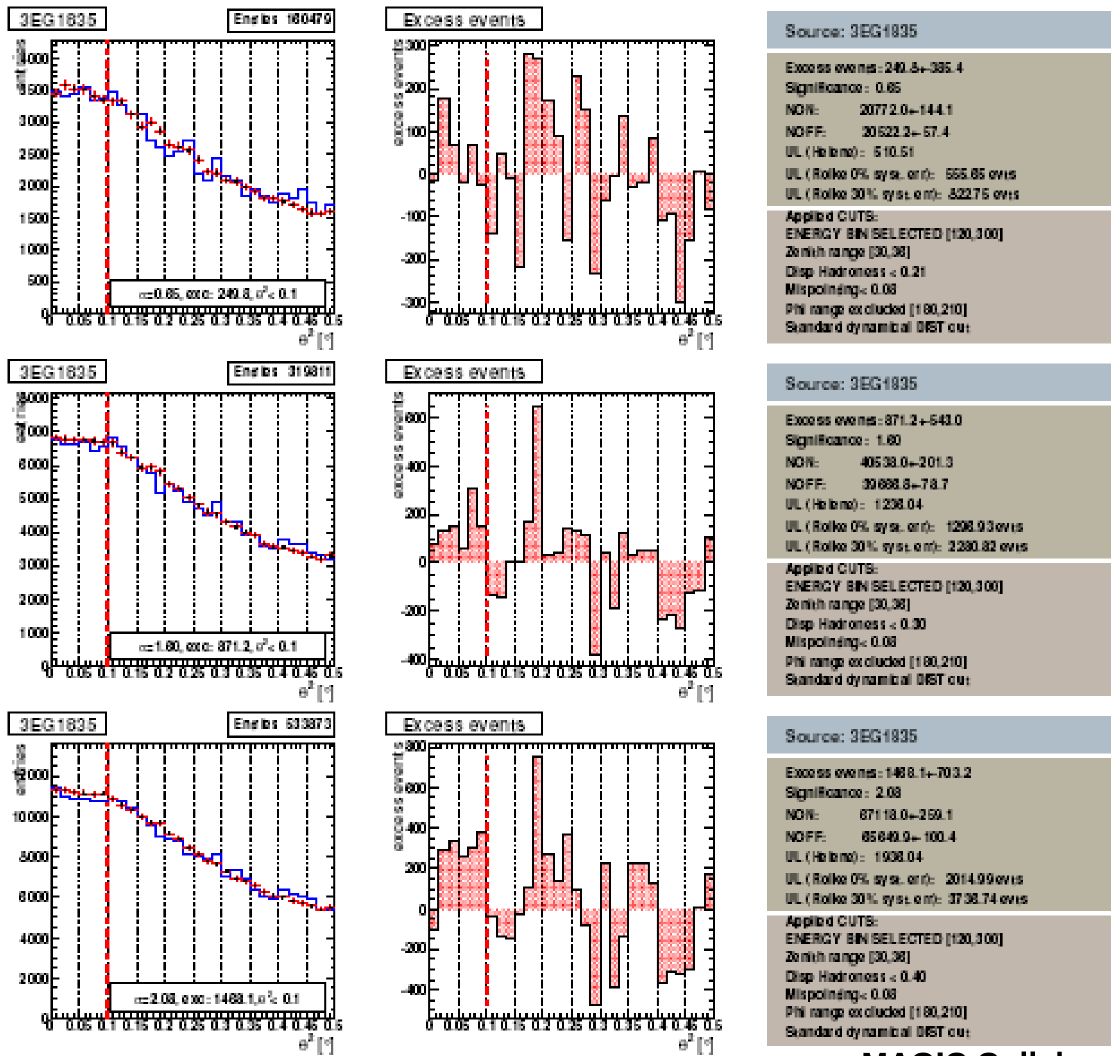

MAGIC Collaboration

HINT OF AN ECCESS: α – PLOT, θ^2 – PLOT (120–300 GeV, 30–36 ZA)

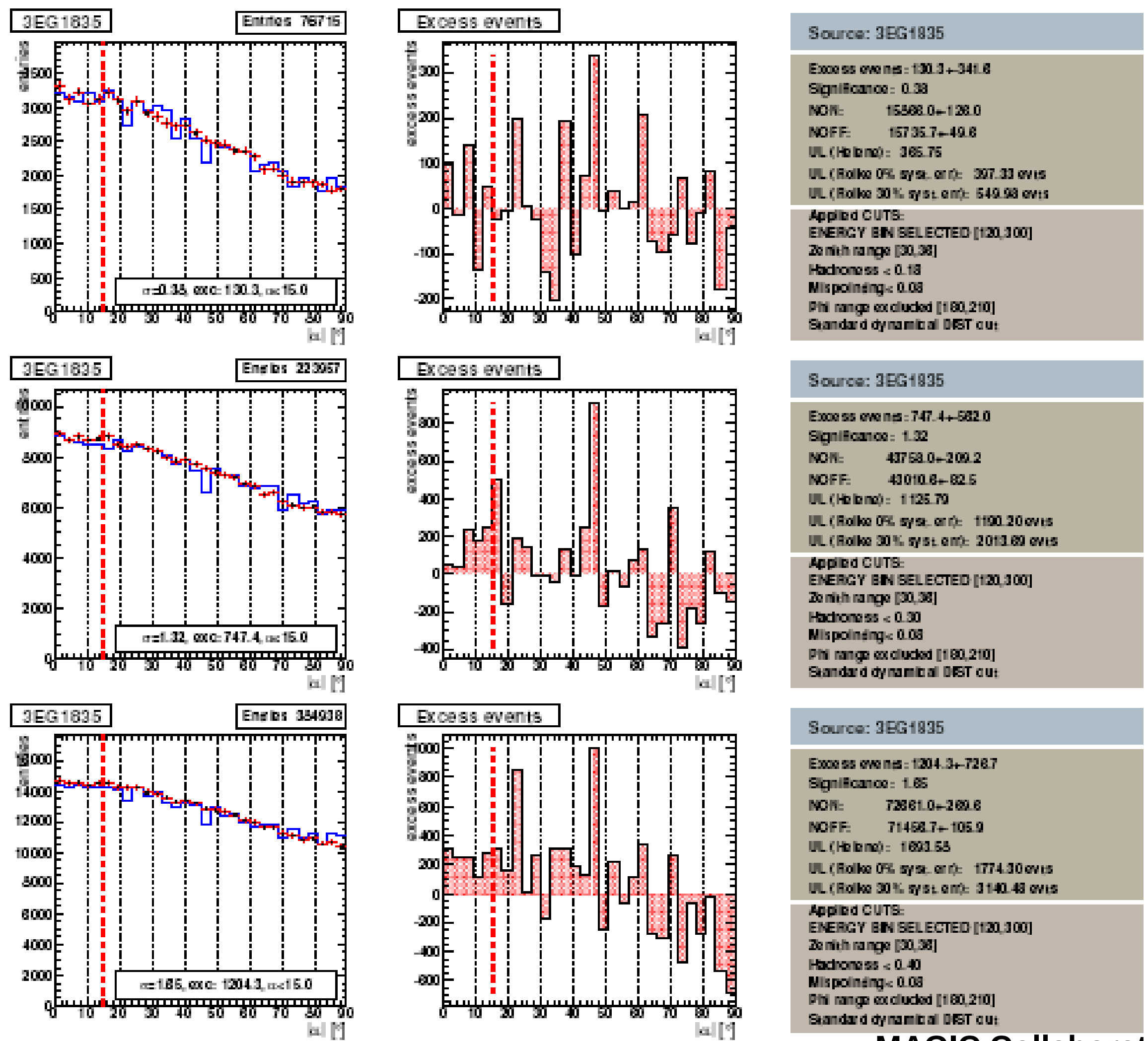

MAGIC Collaboration

3EG_J1835+5918 SKYMAP with DISP

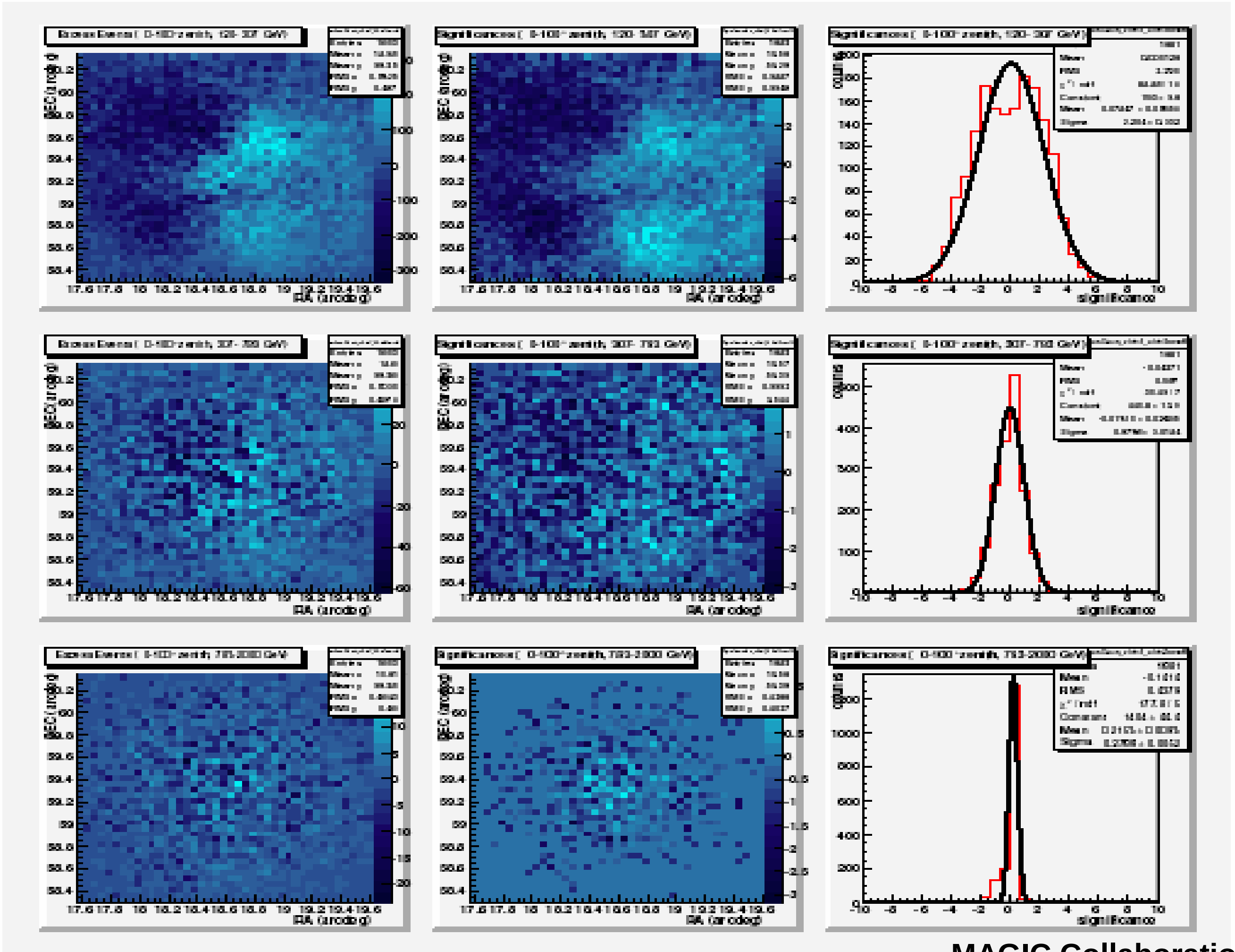

MAGIC Collaboration

DIFFERENTIAL SPECTRUM OF 3EG_J1835+5918

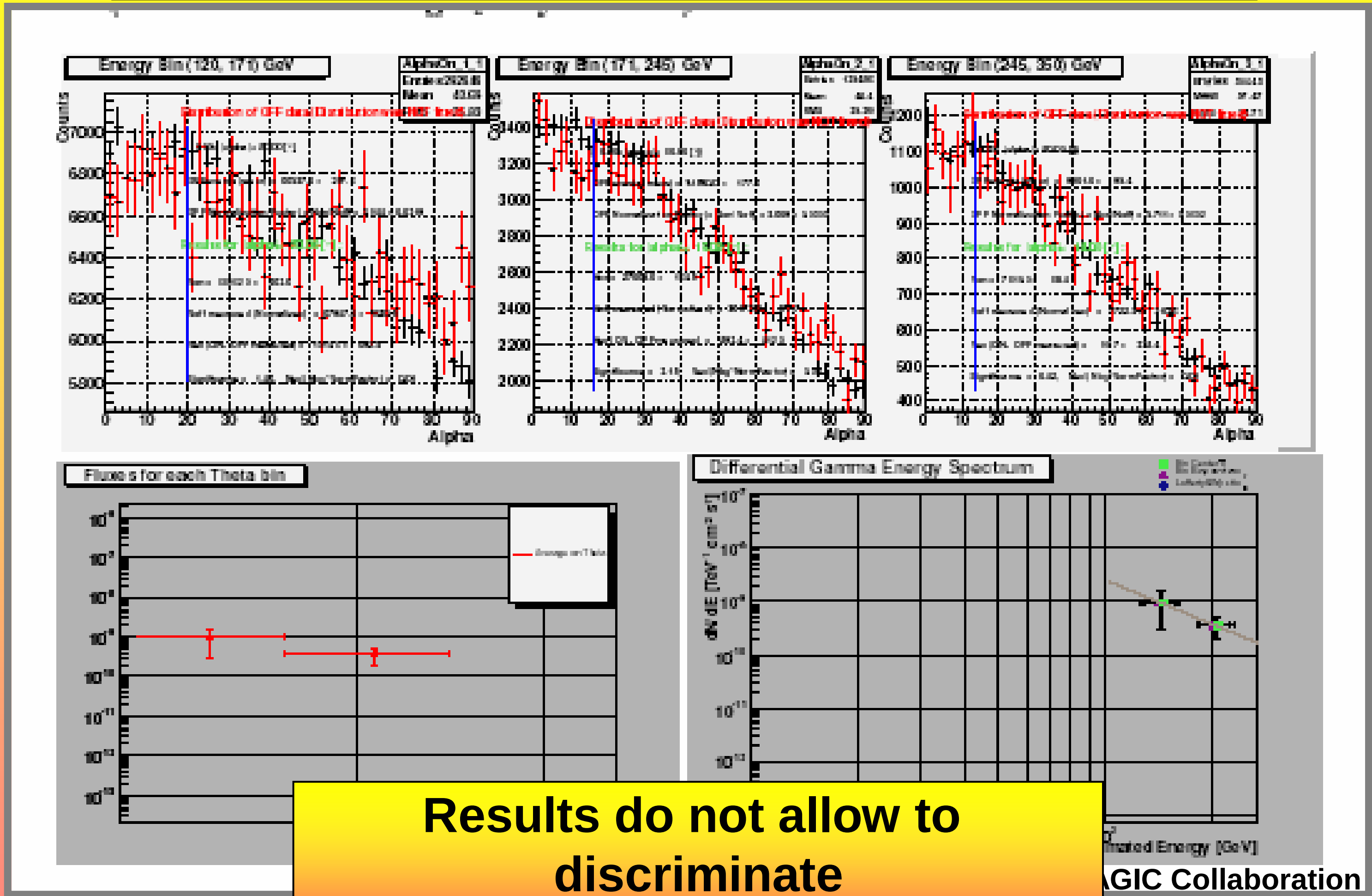

Results do not allow to discriminate among source models

The Draco dwarf galaxy

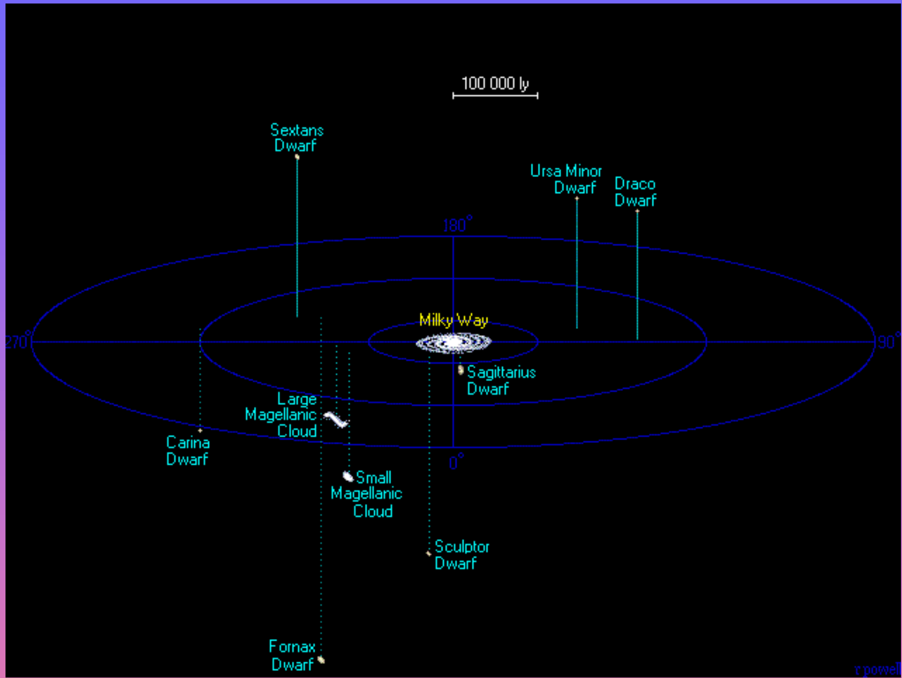

MAIN PROPERTIES OF DRACO:

Type	dE0 pec, dwarf
Right Ascension	$17^{h}\ 20.1^{m}$
Declination	$57^\circ\ 55'$
Distance	80 kpc
Apparent Magnitude	+9.9
Apparent Dimension	$51' \cdot 31'$

Outlook for MAGIC observations:

- **northern emisphere location**
- **ZA ~ 29° → E_{th} ~ 100 GeV**
- **Background:**

$$\frac{dN_{had}}{d\Omega}(E > E_0) = 6.1 \cdot 10^{-3}\, \varepsilon_{had} \left(\frac{E_0}{1\,\mathrm{GeV}}\right)^{-1.7} \mathrm{cm}^{-2}\,\mathrm{s}^{-1}\,\mathrm{sr}^{-1}$$

$$\frac{dN_{el}}{d\Omega}(E > E_0) = 3.0 \cdot 10^{-2} \left(\frac{E_0}{1\,\mathrm{GeV}}\right)^{-2.3} \mathrm{cm}^{-2}\,\mathrm{s}^{-1}\,\mathrm{sr}^{-1}$$

The observation of Draco with MAGIC

Simulation Predictions:

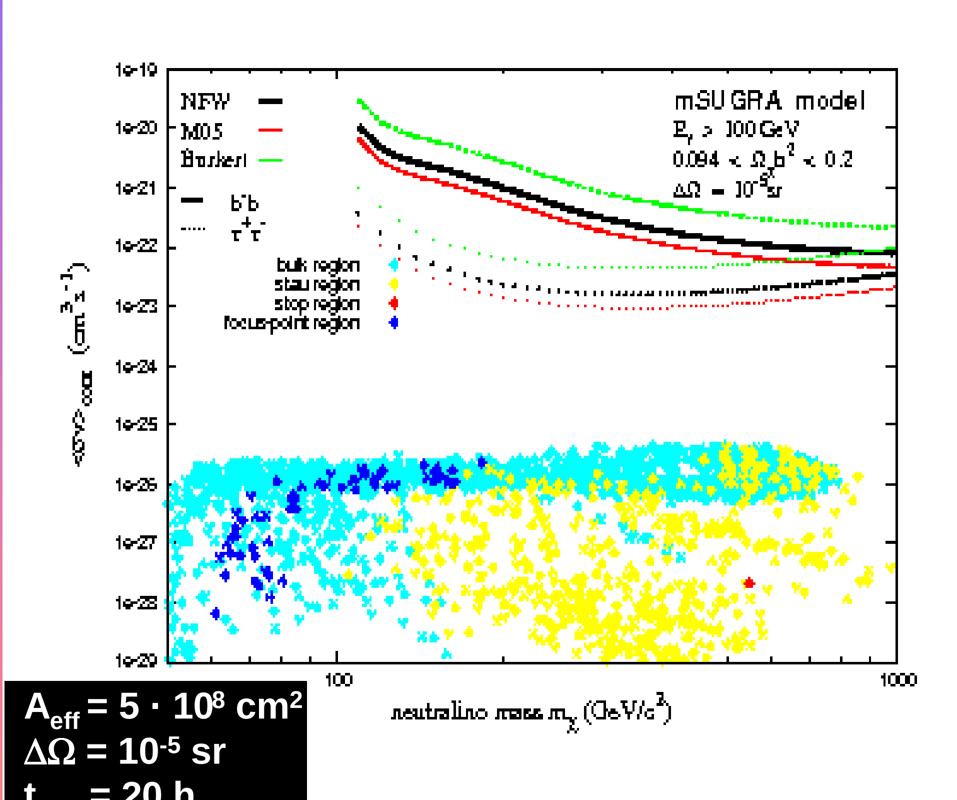

$A_{eff} = 5 \cdot 10^8$ cm^2
$\Delta\Omega = 10^{-5}$ sr
t_{obs} = 20 h
5σ level

Observation:

Between May and June, 2006:
20 hours **ON**
5 hours **OFF**

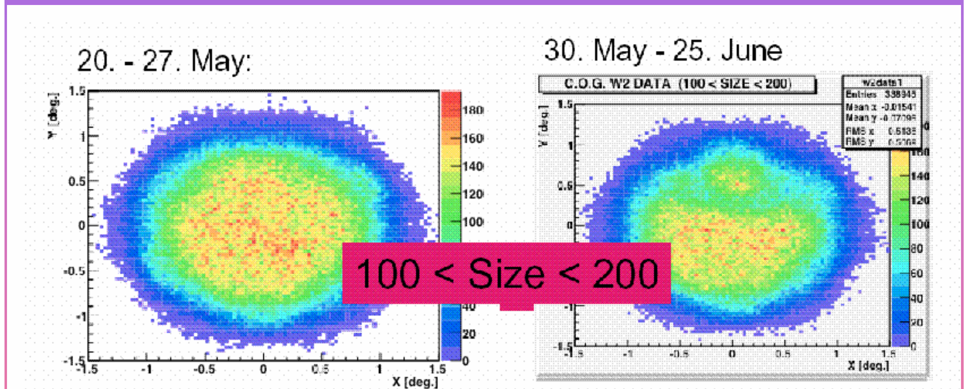

MAGIC Collaboration

Two different data sets:

1. **one not affected by camera inhomogeneity**
2. **another taken after fixing hardware problems**

The baryonic vs dark matter luminosity of star-forming galaxies

- **In a given galaxy, the higher the gas mass, the higher the star formation rate (SFR), the more frequent the supernova explosions, hence the more intense the TeV emission.**
- **Reversing the argument, TeV emission gauges SFR.**

<u>Properties of the TeV sources in our Galaxy:</u>

- **In Galactic plane ($|l| \leq 30°$, $|b| \leq 30°$) : 14 TeV sources (HESS, MAGIC)**
  Proposed counterparts: SNR, PWN, XRB, PSR, BH.

  (In any case, the progenitors are supposed to be massive, bright and short-lived stars)

The baryonic vs dark matter luminosity of star-forming galaxies

- **In a given galaxy, the higher the gas mass, the higher the star formation rate (SFR), the more frequent the supernova explosions, hence the more intense the TeV emission.**
- **Reversing the argument, TeV emission gauges SFR.**

TEV POINT SOUCES:

- A complete sample of sources.
- Collective photon luminosity: $\mathbf{L^{TP}_{\geq 0.2\,TeV} = 2.4 \cdot 10^{36}\ ph\ s^{-1}}$.
- Extrapolation to a thin exponential disk: $\sigma(R) \propto e^{-R/R_d}$, with $R_d = 2.25$ **kpc:**

$$L^{TP}_{\geq 0.2\,TeV} = 4.27 \cdot 10^{36}\ ph\ s^{-1};$$

$$L^{TP}_{\geq 0.2\,TeV}(\varepsilon) \sim 6.3 \cdot 10^{35}\ (\varepsilon/TeV)^{-2.4}\ ph\ s^{-1}\ TeV^{-1} \qquad (1)$$

TeV point sources as CR accelerators:

Assuming that the observed gamma-ray photons are of hadronic origin:

$$L_{\geq\varepsilon} = \int_V g_{\geq\varepsilon}\, n U_{CR}\, dV \;\; \mathrm{ph\,s^{-1}} \qquad (2)$$

Baryonic luminosity

TeV point emission from starburst galaxies:

- **In star-forming galaxies, the collective TP emission is an indicator of the current SFR**
- **Assume that various terms in Eq. (2) scale with SFR: $U_{CR} \propto$ SFR,**

Schmidt law: **$n \propto \mathrm{SFR}^{1/\eta}$, with $\eta = 1.5$**

- **SFR ~ L_{FIR}** **scaling relation:**

$$\Phi^{TP}_{\geq 0.2\,\mathrm{TeV}}(\varepsilon) \approx 6.3\cdot 10^{35}\left(\frac{\varepsilon}{\mathrm{TeV}}\right)^{-2.4}\cdot\left(\frac{L_{\mathrm{FIR}}}{4.4\cdot 10^{43}\,\mathrm{erg\,s^{-1}}}\right)^{1+\frac{1}{\eta}} \mathrm{ph\,s^{-1}\,TeV^{-1}}$$

an order of magnitude

Diffuse TeV radiation in starburst galaxies:

$$L^{\mathrm{gas}}_{\geq\varepsilon} = 2\cdot 10^{37}\left(\frac{\varepsilon}{\mathrm{TeV}}\right)^{-1.1}\cdot\left(\frac{U_{\mathrm{CR}}}{\mathrm{eV\,cm^{-2}}}\right)\cdot\left(\frac{M_{\mathrm{gas}}}{10^9 M_{\mathrm{sun}}}\right)\cdot\left(\frac{L_{\mathrm{FIR}}}{4.4\cdot 10^{43}\,\mathrm{erg\,s^{-1}}}\right)^{1+\frac{1}{\eta}} \mathrm{ph\,s^{-1}}$$

Non-baryonic luminosity

Dark matter annihilation into TeV gamma rays: $\tau^+\tau^-$, b^-b, t^-t, W^+W^-, ZZ

- **smooth component**
- **subhalo component**

TeV gamma rays from the Andromeda galaxy

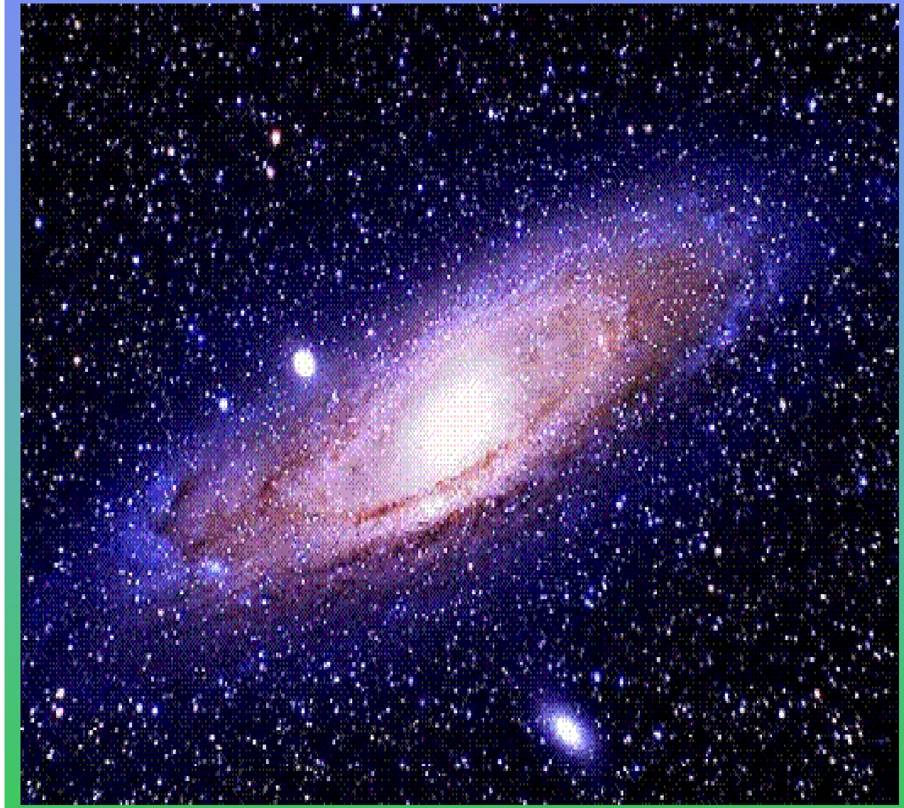

MAIN PROPERTIES OF ANDROMEDA:

Type	Sb
Right Ascension	$00^{\mathrm{h}}\ 42.7^{\mathrm{m}}$
Declination	$41^\circ\ 16'$
Zenith distance at culmination	13°
Distance	700–889 kpc
Radius	33.7 kpc
Redshift	-0.001
Apparent magnitude	$+3.4$
Absolute magnitude	-21.4
Total mass	$1.2 \cdot 10^{12}\ \mathrm{M}_\odot$
Mass/Luminosity ratio	12 ± 1
Apparent Dimension	$3.2^\circ \cdot 1.0^\circ$

TeV gamma rays from the Andromeda galaxy

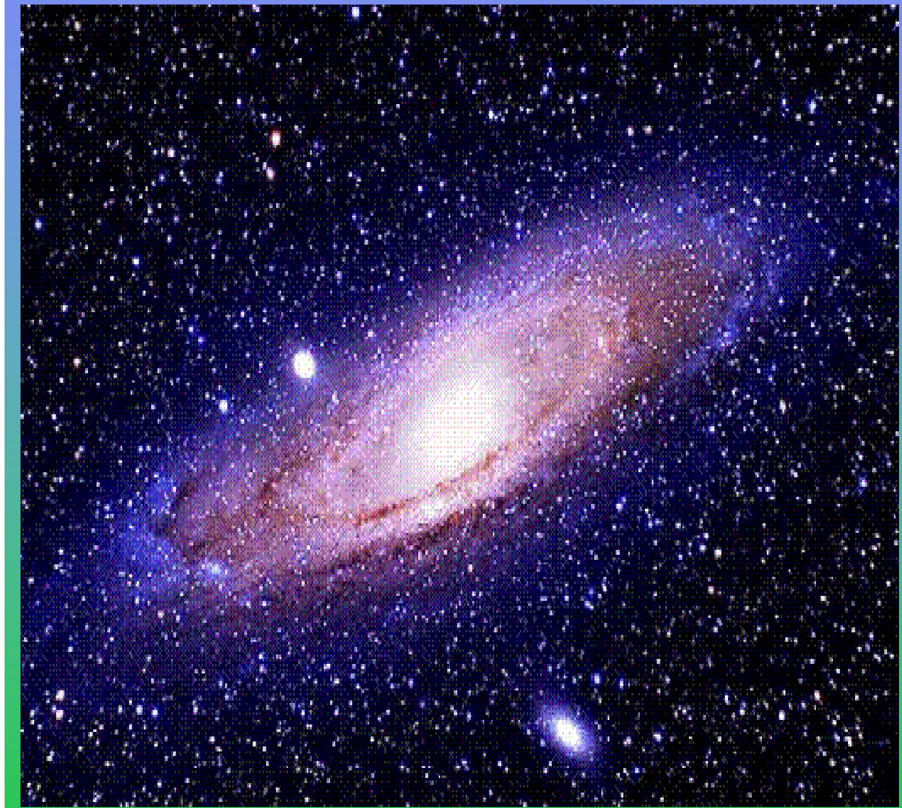

First observation by HEGRA:

- 20.1 hours
- ZA ≤ 25°
- **no excess of signal over a few percent of Crab**
- **upper limits at 1 TeV: 0.033 CU (center),**
  0.3 CU (outer)

A new observation with MAGIC ?

- 30 hours
- 0° ≤ ZA ≤ 30°
- **new upper limits (5σ):**

E > 1 TeV: 0.029 CU = $5.2 \cdot 10^{-13}$ ph cm^{-2} s^{-1}

E > 200 GeV: 0.022 CU = $5.2 \cdot 10^{-12}$ ph cm^{-2} s^{-1}

TeV gamma rays from the Andromeda galaxy

Expected baryonic background:

$\Phi_{\geq 0.2\ \mathrm{TeV}} \sim 2.5 \cdot 10^{-15}$ **ph cm^{-2} s^{-1} by TPS**

$\Phi_{\geq 0.2\ \mathrm{TeV}} \sim 7 \cdot 10^{-14}$ **ph cm^{-2} s^{-1} DIFFUSE**

Extended object (fluxes averaged on the MAGIC $\Delta\Omega = 10^{-5}$ **sr**):

TeV dark matter

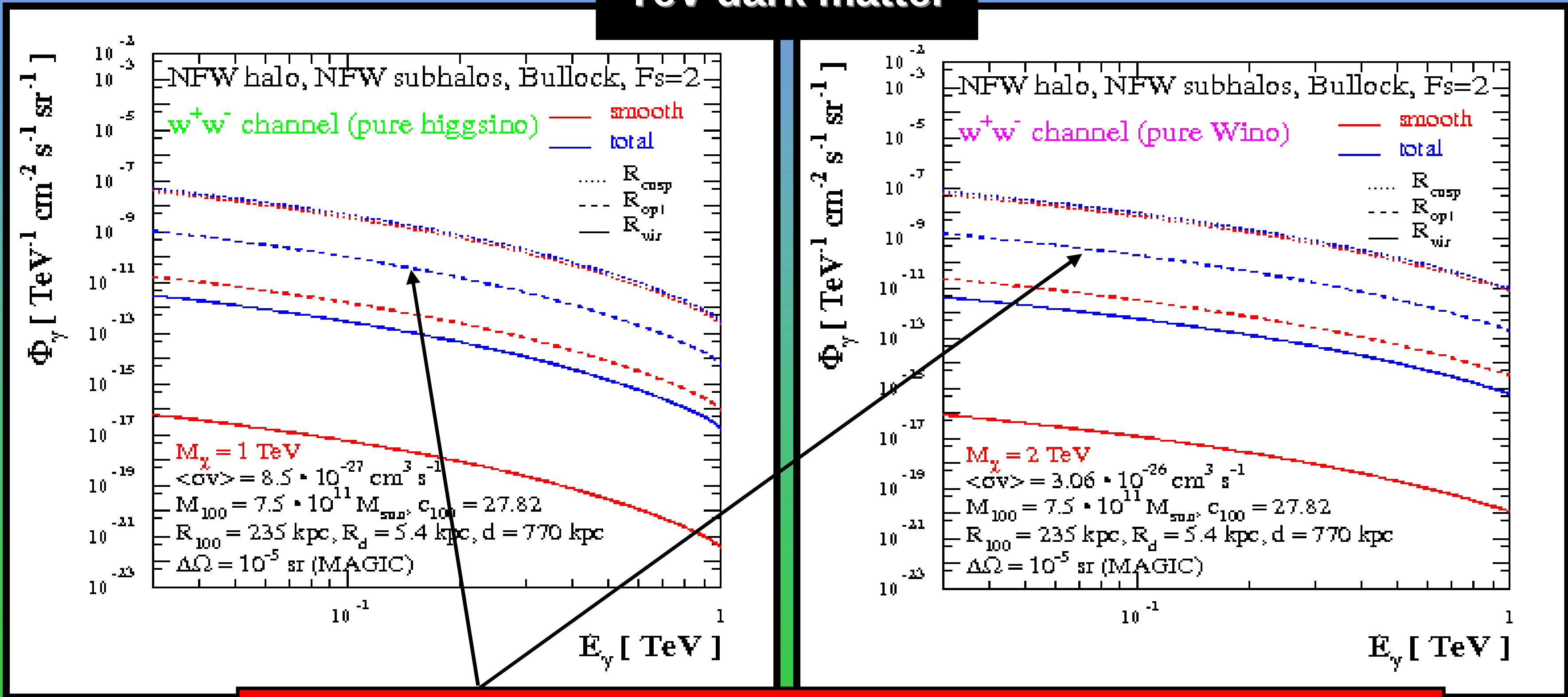

possible to separate the two contributions at the optical radius

TeV gamma rays from the Andromeda galaxy

Expected baryonic background:

$\Phi_{\geq 0.2\ \mathrm{TeV}}$ **~ 2.5 · 10^{-15} ph cm^{-2} s^{-1} by TPS**

$\Phi_{\geq 0.2\ \mathrm{TeV}}$ **~ 7 · 10^{-14} ph cm^{-2} s^{-1} DIFFUSE**

Extended object (fluxes averaged on the MAGIC $\Delta\Omega = 10^{-5}$ **sr**):

Pros:

low density matter, both baryonic and dark

Optical radius: $R_{opt} = 3R_d$

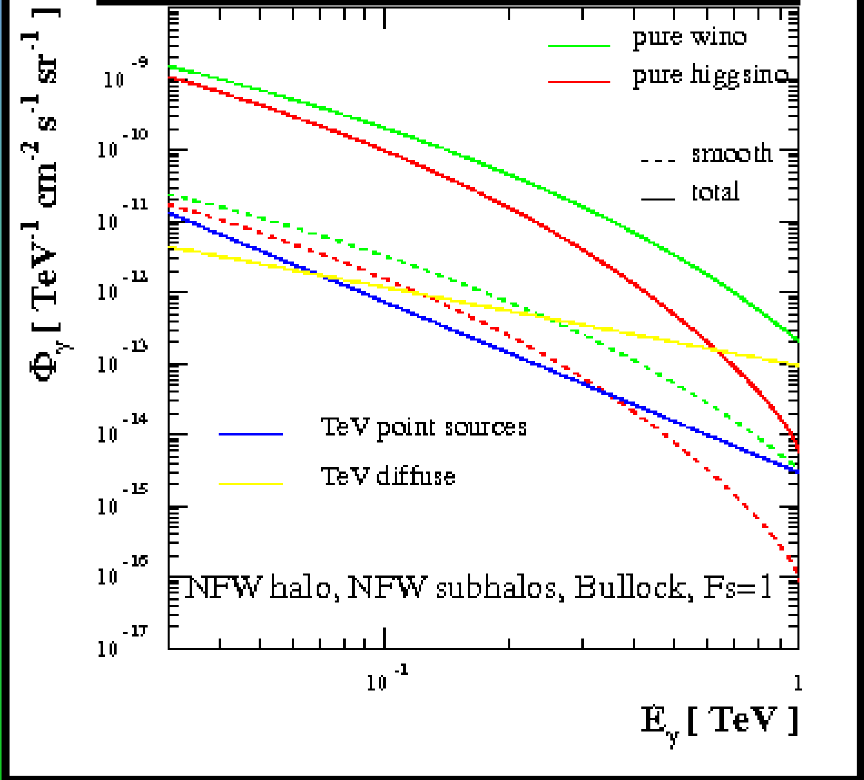

Cons:

optimal rejection of baryonic background

possibility to infer existence of subhalos

Conclusions:

An enhancement of more than one order of magnitude in gamma-ray signal is found when considering a more realistic DM distribution.

The unidentified EGRET source 3EG_J1835+5918 as a DM clump?
Very low probability!

No clear indication of a signal from 3EG_J1835+5918 by MAGIC.
Alternative explanations: a Geminga-like pulsar?

Prospects for detecting gamma-rays from Andromeda:
Is there any chance to infer existence of subhalos with next generation telescopes?

And looking to the future...

THE END